



## Pericyte-derived Bone Morphogenetic Protein 4 Underlies White Matter Damage after Chronic Hypoperfusion

Journal:	<i>Brain Pathology</i>
Manuscript ID	BPA-16-10-RA-161.R2
Wiley - Manuscript type:	Research Article
Date Submitted by the Author:	n/a
Complete List of Authors:	Uemura, Maiko; Kyoto University Graduate School of Medicine, Department of Neurology Ihara, Masafumi; National Cerebral and Cardiovascular Center Hospital, Stroke and Cerebrovascular Disease Maki, Takakuni; Kyoto University Graduate School of Medicine, Department of Neurology Nakagomi, Takayuki; Hyogo College of Medicine, Institute for Advanced Medical Sciences Kaji, Seiji; Kyoto University Graduate School of Medicine, Department of Neurology Uemura, Kengo; Ishiki Hospital, Department of Neurology Matsuyama, Tomohiro; Hyogo College of Medicine, Institute for Advanced Medical Sciences Kalaria, Raj; Newcastle University, Campus for Ageing and Vitality, Neuroscience Kinoshita, Ayae; Kyoto University Graduate School of Medicine, School of Human Health Sciences Takahashi, Ryosuke; Kyoto University Graduate School of Medicine, Department of Neurology
Keywords:	BMP4, pericyte, small vessel disease, chronic hypoperfusion, oligodendrocyte precursor cell
Note: The following files were submitted by the author for peer review, but cannot be converted to PDF. You must view these files (e.g. movies) online.	
Supplementary movie 1_Proliferation Assay.mp4 Supplementary movie 2_Differentiation Assay.mp4	

SCHOLARONE™  
Manuscripts

1  
2  
3  
4  
5 **1 Pericyte-derived Bone Morphogenetic Protein 4 Underlies White Matter Damage**  
6  
7 **2 after Chronic Hypoperfusion**  
8  
9  
10  
11  
12  
13  
14  
15  
16  
17  
18  
19  
20  
21  
22  
23

24  
25  
26  
27  
28  
29  
30  
31  
32  
33  
34  
35  
36  
37  
38  
39  
40  
41  
42  
43  
44  
45  
46  
47  
48  
49  
50  
51  
52  
53  
54  
55  
56  
57  
58  
59  
60

4 Maiko T Uemura, M.D.<sup>1</sup>, Masafumi Ihara, M.D., Ph.D., F.A.C.P.<sup>2\*</sup>, Takakuni Maki,  
5 M.D., Ph.D.<sup>1</sup>, Takayuki Nakagomi M.D., Ph.D.<sup>3</sup>, Seiji Kaji, M.D.<sup>1</sup>, Kengo Uemura M.D.,  
6 Ph.D.<sup>4</sup>, Tomohiro Matsuyama, M.D., Ph.D.<sup>3</sup>, Raj N. Kalaria, Ph.D, FRCP<sup>5</sup>, Ayae  
7 Kinoshita, M.D., Ph.D.<sup>6</sup>, Ryosuke Takahashi, M.D., Ph.D.<sup>1</sup>

9 <sup>1</sup>Department of Neurology, Kyoto University Graduate School of Medicine, Kyoto,  
10 Japan

11 <sup>2</sup>Department of Stroke and Cerebrovascular Diseases, National Cerebral and  
12 Cardiovascular Center Hospital, Osaka, Japan

13 <sup>3</sup>Institute for Advanced Medical Sciences, Hyogo College of Medicine, Hyogo, Japan

14 <sup>4</sup>Department of Neurology, Ishiki Hospital, Kagoshima, Japan

15 <sup>5</sup>Institute of Neuroscience, Newcastle University, Campus for Ageing and Vitality,  
16 Newcastle upon Tyne, UK

17 <sup>6</sup>School of Human Health Sciences, Kyoto University Graduate School of Medicine,  
18 Kyoto, Japan

19  
20 \*Correspondence to: Masafumi Ihara, MD, PhD, FACP

21 Department of Neurology, National Cerebral and Cardiovascular Center Hospital,  
22 Osaka, Japan

23 5-7-1 Fujishiro-dai, Suita, Osaka 565-8565, Japan

- 1 FAX: +81-6-6835-5137
- 2 TEL: +81-6-6833-5012
- 3 E-mail address: [ihara@ncvc.go.jp](mailto:ihara@ncvc.go.jp)

For Peer Review Only

1 **Pericyte-derived Bone Morphogenetic Protein 4 Underlies White Matter Damage**  
2 **after Chronic Hypoperfusion**

3

4 Maiko T Uemura, M.D.<sup>1</sup>, Masafumi Ihara, M.D., Ph.D., F.A.C.P.<sup>2\*</sup>, Takakuni Maki,  
5 M.D., PhD<sup>1</sup>, Takayuki Nakagomi M.D., Ph.D.<sup>3</sup>, Seiji Kaji, M.D.<sup>1</sup>, Kengo Uemura M.D.,  
6 Ph.D.<sup>4</sup>, Tomohiro Matsuyama, M.D., Ph.D.<sup>3</sup>, Raj N. Kalaria, Ph.D, FRCP<sup>5</sup>, Ayae  
7 Kinoshita, M.D., Ph.D.<sup>6</sup>, Ryosuke Takahashi, M.D., Ph.D<sup>1</sup>

8

9 <sup>1</sup>Department of Neurology, Kyoto University Graduate School of Medicine, Kyoto,  
10 Japan

11 <sup>2</sup>Department of Stroke and Cerebrovascular Diseases, National Cerebral and  
12 Cardiovascular Center Hospital, Osaka, Japan

13 <sup>3</sup>Institute for Advanced Medical Sciences, Hyogo College of Medicine, Hyogo, Japan

14 <sup>4</sup>Department of Neurology, Ishiki Hospital, Kagoshima, Japan

15 <sup>5</sup>Institute of Neuroscience, Newcastle University, Campus for Ageing and Vitality,  
16 Newcastle upon Tyne, UK

17 <sup>6</sup>School of Human Health Sciences, Kyoto University Graduate School of Medicine,  
18 Kyoto, Japan

19

20 \*Correspondence to: Masafumi Ihara, MD, PhD, FACP

21 Department of Neurology, National Cerebral and Cardiovascular Center Hospital,  
22 Osaka, Japan

23 5-7-1 Fujishiro-dai, Suita, Osaka 565-8565, Japan

- 1 FAX: +81-6-6835-5137
- 2 TEL: +81-6-6833-5012
- 3 E-mail address: [ihara@ncvc.go.jp](mailto:ihara@ncvc.go.jp)

1 **Abstract**

2

3 Subcortical small vessel disease (SVD) is characterized by white matter damage  
4 resulting from arteriolosclerosis and chronic hypoperfusion. Transforming growth factor  
5 beta 1 (TGFB1) is dysregulated in the hereditary SVD, CARASIL (cerebral autosomal  
6 recessive arteriopathy with subcortical infarcts and leukoencephalopathy). However,  
7 very little is known about the role of the largest group in the TGFB superfamily – the  
8 bone morphogenetic proteins (BMPs) – in SVD pathogenesis. The aim of this study was  
9 to characterize signaling abnormalities of BMPs in sporadic SVD. We examined  
10 immunostaining of TGFB1 and BMPs (BMP2/BMP4/ BMP6/ BMP7/ BMP9) in a total  
11 of 19 post-mortem human brain samples as follows: 7 SVD patients (4 males, 76–90  
12 years old); 6 Alzheimer’s disease (AD) patients (2 males, 67–93 years old); and 6  
13 age-matched disease controls (3 males, 68–78 years old). We subsequently investigated  
14 the effects of oxygen-glucose deprivation and BMP4 addition on cultured cells.  
15 Furthermore, adult mice were subjected to continuous intracerebroventricular infusion  
16 of the BMP antagonist, noggin, followed by chronic cerebral hypoperfusion using  
17 bilateral common carotid artery stenosis. In the SVD cases, BMP4 was highly expressed  
18 in white matter pericytes. Oxygen-glucose deprivation induced BMP4 expression in  
19 cultured pericytes *in vitro*. Recombinant BMP4 increased the number of cultured  
20 endothelial cells and pericytes and converted oligodendrocyte precursor cells into  
21 astrocytes. Chronic cerebral hypoperfusion *in vivo* also upregulated BMP4 with  
22 concomitant white matter astrogliogenesis and reduced oligodendrocyte lineage cells,  
23 both of which were suppressed by intracerebroventricular noggin infusion. Our findings  
24 suggest ischemic white matter damage evolves in parallel with BMP4 upregulation in

1 pericytes. BMP4 promotes angiogenesis, but induces astrogliogenesis at the expense of  
2 oligodendrocyte precursor cell proliferation and maturation, thereby aggravating white  
3 matter damage. This may explain white matter vulnerability to chronic hypoperfusion.  
4 The regulation of BMP4 signaling is a potential therapeutic strategy for treating SVD.

## 6 **Introduction**

7  
8 Vascular cognitive impairment develops as a consequence of various types of  
9 cerebrovascular alterations. Subcortical white matter changes caused by small vessel  
10 alterations are frequently observed in vascular cognitive impairment and are referred to  
11 as subcortical ‘small vessel disease (SVD)’ (39). Disturbances in cerebrospinal fluid  
12 production (40), cerebral edema (22), breakdown of the blood–brain barrier and  
13 increased permeability (21, 54), oxidative stress (4) and inflammation have been cited  
14 as important causes in the development of white matter changes (19). However, the  
15 exact mechanisms have yet to be fully elucidated. Recent studies have noted that  
16 attenuations of vasculature and white matter are also frequently observed in other  
17 neurodegenerative disorders, especially in Alzheimer’s disease (AD) (46, 59). However,  
18 vascular risk factors are related to a lesser degree to a pure type of AD (10, 38) or mixed  
19 type (AD with vascular pathology) dementia (23) compared with vascular cognitive  
20 impairment. The involvement of different etiologies has been suggested in white matter  
21 damage between SVD and AD (13, 20). Therefore, clarification of causative factors that  
22 underlie various forms of white matter changes should enable the development of novel  
23 strategies for tackling cognitive impairment.

24 There are several recognized forms of inherited SVD (9), including CARASIL (cerebral

1 autosomal recessive hereditary cerebral artery disease and arteriosclerosis with  
2 subcortical infarcts and leukoencephalopathy). The gene responsible for CARASIL is  
3 *HTRA1* (high-temperature requirement A 1), and the resultant upregulation of  
4 transforming growth factor beta (TGFB) family signaling is postulated to underlie the  
5 small vessel changes observed in CARASIL (18). The TGFB superfamily also includes  
6 the bone morphogenetic protein (BMP) family proteins.

7 BMPs are involved in oligovascular pathologies in the ischemic brain, in addition to  
8 their physiological roles in embryonic and bone tissues, In an ischemic intrauterine  
9 growth retardation model, oxidative stress upregulates BMP4 and mediates  
10 periventricular white matter injury with a paucity of mature oligodendrocytes and  
11 hypomyelination, while BMP deletion reverses these defects (36). In neonatal mouse  
12 brains, BMP4 expression increases as a consequence of global hypoxia-ischemia, while  
13 the BMP antagonist noggin protects the white matter against damage (12). Furthermore,  
14 in adult mouse brains with focal cerebral ischemia, overexpressed noggin reduces  
15 infarct volume and motor deficits (44). These experimental results highlight the  
16 potential of BMP antagonism in the treatment of ischemic demyelinating disorders.

17 Nevertheless, the exact role of BMP family members remains poorly understood in the  
18 context of chronic hypoperfusion in the adult human brain. Therefore, the present study  
19 explored the underlying etiology of white matter abnormalities, specifically focusing on  
20 BMP expression through the use of postmortem human brains, cultured cells exposed to  
21 oxygen-glucose deprivation (OGD), and chronic hypoperfusion mouse brains.

22

## 23 **Materials and Methods**

24



## 1 **Experimental design of postmortem brain material**

2  
3 Study samples were selected from 371 autopsied brains retained at Kyoto University  
4 Hospital from 1983 to 2009. This collection was approved by the institutional research  
5 committee, Kyoto University Graduate School and Faculty of Medicine, Ethics  
6 Committee. Neuropathological diagnoses were made according to thorough  
7 histopathological examination of extensively sampled brain sections, as previously  
8 described (1, 35). Cases with mixed SVD and AD pathological diagnoses were excluded  
9 to select for brain samples with relatively single processes. We analyzed a total of 19  
10 postmortem brain samples as follows: 7 SVD patients (4 males, 76–90 years old, brain  
11 weight  $1101 \pm 89.9$  g); 6 AD patients (2 males, 67–93 years old, brain weight  $1056 \pm$   
12  $67.7$  g); and 6 age-matched disease controls (3 males, 68–78 years old, brain weight  
13  $1190 \pm 113.7$  g). Table 1 provides demographics and pathological features of the 19  
14 subjects. The clinical diagnosis of dementia met the criteria of the Diagnostic and  
15 Statistical Manual of Mental Disorders IV (2). The AD neuropathological diagnoses  
16 were made according to the presence of frequent senile plaques in the neocortex (32),  
17 and no less than stage V of Braak stage of neurofibrillary tangles (6, 7). The diagnosis  
18 of SVD, or subcortical ischemic vascular dementia was clinically made (5) and was  
19 retrospectively found to meet the pathological criteria outlined by Kalaria *et al.* (24).  
20 Two observers (M.U. and M.I.) individually assessed senile plaque and neurofibrillary  
21 tangle stages, and if required, a joint assessment was scrutinized under a two-headed  
22 microscope.

## 24 **Tinctorial staining and immunohistochemistry for postmortem human brain**

1 **samples**

2

3 Six micrometer-thick paraffin-embedded tissue sections were cut from the frontal lobes  
4 at the level of the olfactory bulbs and stained for Luxol fast blue. Some sections were  
5 also incubated with specific primary antibodies (listed in Supplementary Table 1)  
6 overnight at 4°C. Sections were pretreated at 90°C for 20 min in Tris-ethylenediamine  
7 tetraacetic acid (pH 9.0) for actin, alpha 2, smooth muscle, aorta (ACTA2, also known  
8 as  $\alpha$ SMA) and platelet-derived growth factor receptor alpha (PDGFRA), and some were  
9 pretreated at 121°C for 15 min in 0.01 M citrate buffer (pH 6.0) using an autoclave for  
10 BMP2. This was followed by appropriate biotinylated secondary antibody (1:200,  
11 Vector Laboratories, CA, USA) and avidin-biotin-peroxidase complex (1:200, Vector  
12 Laboratories), or polymer Detection System (Histofine Simple Stain MAX PO MULTI,  
13 Nichirei Biosciences, Tokyo, Japan) application. Between steps, the sections were  
14 washed three times for 5 min with 0.1 M phosphate-buffered saline (PBS, pH 7.4) and  
15 visualized using 0.01% diaminobenzidine tetrahydrochloride and 0.003% H<sub>2</sub>O<sub>2</sub> in 50  
16 mM Tris-HCl (pH 7.5).

17 For triple-immunofluorescence, deparaffinized sections were incubated with a mixture  
18 of primary antibodies overnight at 4°C, followed by Alexa Fluor 488, 594, and 647  
19 conjugated secondary antibodies (1:200, Invitrogen, CA, USA) for 2 h at room  
20 temperature.

21 The images of interest were captured with a microscope (BZ-X700, Keyence, Osaka,  
22 Japan) or a confocal laser-scanning microscope (FV1000, Olympus, Tokyo, Japan).

23

24 **Assessment of myelin density or immunohistochemical staining**

1

2 Myelin density was assessed using immunohistochemistry and myelin index as  
3 previously described (20, 58). Briefly, to determine the myelin index, the white matter  
4 was automatically outlined using the wand tool of Image J. If the border between the  
5 cortex and white matter was obscured due to severe myelin loss, the white matter was  
6 manually outlined using the semiautomatic trace tool instead of the wand tool. The  
7 detected range of gray levels within the white matter, corresponding to the staining  
8 intensity, from 0–127 (0, white; 255, black) was divided into four quartiles (the first  
9 quartile 0–29, the second 30–62, the third 63–94, and the fourth 95–127). The percent  
10 area for each quartile was calculated. The median gray level of each quartile (14.5, 46.0,  
11 78.5, and 111.0), an estimated staining intensity, was then multiplied by percent area in  
12 each quartile and summed up, providing the total myelin index (Figure 1A).

13 For immunohistochemical staining, images from 15–20 randomly selected ROIs were  
14 captured. The images were then converted into 8-bit grayscale, binarized by threshold  
15 using the Triangle Method, and the area above threshold measured using Fiji and Image  
16 J. For quantification of BMP4 immunoreactivity in PDGFRB- and ACTA2-positive  
17 cells, images of PDGFRB or ACTA2 immunostaining were firstly converted into  
18 binarized images using the Triangle Method and the area above threshold was selected.  
19 The selected area was applied to the same section with BMP4 immunostaining, and the  
20 mean intensity and percent area of BMP4 in the selected area measured.

21 The above analyses were performed blinded to the diagnosis by labeling sections with  
22 arbitrary numbers.

23

1 **Cell culture**

2

3 Mouse brain vascular pericytes (1200, ScienCell, Carlsbad, CA, USA) and human brain  
4 microvascular endothelial cells (ACBRI, HBMD, Cell Systems, Kirkland, WA, USA)  
5 were cultured with pericyte medium (1201, ScienCell) or endothelial cell growth  
6 medium (CC-3156 and CC-4147, Lonza, Basel, Switzerland) containing 10% fetal  
7 bovine serum and 1% penicillin/streptomycin. Endothelial cells were placed on  
8 pre-coated dishes with 3.2% bovine collagen type IV alpha 1 chain (COL4A1)  
9 (A1064401, Invitrogen) in PBS. Oligodendrocyte precursor cells (OPCs) were isolated  
10 from cerebral cortices from 1–2-days-old Sprague Dawley rats as previously described  
11 (8, 30).

12

13 **Oxygen–glucose deprivation**

14

15 Upon confluency, pericyte media were replaced with glucose- and serum-free pericyte  
16 media. The following day, culture plates were placed into a hypoxic culture kit  
17 (BIONIX II, Sugiyama-Gen, Tokyo, Japan) with 5% O<sub>2</sub> and 3% CO<sub>2</sub>, and incubated at  
18 37 °C for 1, 2, and 3 days.

19

20 **RT-PCR**

21

22 After preparing the cell lysate, mRNA was rapidly purified using the RNeasy Plus Mini  
23 Kit (74136, Qiagen, Hilden, Germany) and subjected to reverse  
24 transcriptase-polymerase chain reaction (RT-PCR) analysis using appropriate primers

1 (listed in Supplementary Table 2).

2

### 3 **BMP4 and noggin treatment**

4

5 The media were replaced with new medium with or without recombinant human BMP4  
6 (1 or 10 ng/ml, 314-BP, R&D systems) and/or recombinant human noggin (100 ng/ml  
7 for proliferation assay and 500 ng/ml for differentiation assay; 120-10C, PeproTech, IL,  
8 USA). The cells treated with both BMP4 and noggin were pretreated with only noggin  
9 (100 ng/ml for proliferation assay and 500 ng/ml for differentiation assay) for 2 h.

10

### 11 **WST-8 assay**

12

13 Two days after BMP4 and/or noggin administration, 1% of  
14 2-(2-methoxy-4-nitrophenyl)-3-(4-nitrophenyl)-5-(2,4-disulfophenyl)-2H-tetrazolium,  
15 monosodium salt solution (WST-8, 07553-44, Nacalai tesque, Kyoto, Japan) was added  
16 to each medium. Then, the plates were incubated for 1 h at 37°C in the incubator.  
17 Absorbance at 450 nm and 630 nm were measured using a multi-label plate reader  
18 (2030 ARVO X, PerkinElmer, Waltham, MA, USA). The results of absorbance at 450  
19 nm were corrected to absorbance at 630 nm.

20

### 21 **Immunocytochemistry**

22

23 The cells were fixed with 4% paraformaldehyde/PBS for 15 min at room temperature,  
24 treated with 3% bovine serum albumin for 1 h, incubated with primary antibodies (listed

1 in Supplementary Table 3) overnight at 4°C and appropriate secondary antibodies for 2  
2 h at room temperature. Between steps, the cells were washed three times for 5 min with  
3 PBS.

4

#### 5 **Tube formation assay**

6

7 After thawing overnight at 4°C, the matrigel (354230, BD Biosciences, Franklin Lakes,  
8 NJ, USA) was applied on each well of a  $\mu$ -slide (81506, Ibidi, Madison, WI, USA) and  
9 polymerized for 1 h at 37 °C. Then, 50  $\mu$ l of suspension at a density of  $4 \times 10^5$  cells/ml  
10 endothelial cells were added to the matrigel surface. After seeding the cells, the slides  
11 were incubated for 24 h at 37°C. The number of tubes was quantified under a  
12 microscope.

13

#### 14 **OPC proliferation assay and differentiation assay**

15

16 For the proliferation assay, OPCs were cultured with OPC proliferation media  
17 (Neurobasal medium containing 2 mM glutamine, 1% penicillin/streptomycin, 10 ng/ml  
18 platelet-derived growth factor-AA, 10 ng/ml basic fibroblast growth factors, and 2%  
19 B27 supplement). At 30% confluency, the cells were treated with BMP4 and/or noggin  
20 and incubated for two days until harvest and analysis by RT-PCR.

21 For the differentiation assay, when the cells were 70% confluent, the OPC proliferation  
22 media were replaced with OPC differentiation media (Dulbecco's-modified Eagle  
23 Medium containing 1% penicillin/streptomycin, 10 ng/ml ciliary neurotrophic factor, 10  
24 ng/ml triiodothyronine, and 2% B27 supplement). Simultaneously, BMP4 and/or noggin

1 were administered. Four days after treatment, the cells were analyzed by  
2 immunocytochemistry or RT-PCR.

3 Changes in OPC morphologies were captured using a time-lapse camera (BZ-X700,  
4 Keyence).

5

## 6 **Animals and surgical procedure**

7

8 The protocol for this study was approved by the Institutional Animal Care and Use  
9 Committee, Institute of Laboratory Animals Graduate School of Medicine, Kyoto  
10 University.

11 Adult C57BL/6J male mice (10–12 weeks old) were subjected to bilateral common  
12 carotid artery stenosis (BCAS) using microcoils as previously described (n = 6) (29, 48).  
13 Control mice underwent sham surgery (n = 6). Four weeks after BCAS, mice were  
14 euthanized and their brains analyzed by immunohistochemistry and western blot (Figure  
15 6A).

16 In a separate experiment, mice received continuous intracerebroventricular infusion  
17 (cICV) two days prior to BCAS using brain infusion kit 3 (0008851, Alzet, Cupertino,  
18 CA, USA) and micro-osmotic pump (1004, Alzet) under stereotaxis. The pumps were  
19 filled with recombinant human noggin (500 ng/day or 1000 ng/day) in artificial  
20 cerebrospinal fluid (ACSF, 3525, Funakoshi, Tokyo, Japan), or ACSF only, as  
21 previously described (42, 43). Control mice underwent sham surgery (n = 6 for sham  
22 control; n = 6 for BCAS and ACSF; n = 5 for BCAS and noggin 500 ng/day; n = 6 for  
23 BCAS and noggin 1000 ng/day) (Figure 6H).

24

1 **Immunohistochemistry for mouse brain**

2

3 Mice were anesthetized and intracardially perfused with cooled PBS. The brains were  
4 quickly frozen using powdered dry ice. Coronal sections (20- $\mu$ m thick) were cut on a  
5 cryostat at  $-20^{\circ}\text{C}$  and collected onto glass slides. As previously described (47), sections  
6 were fixed with 4% paraformaldehyde/PBS for 15 min and incubated with antibodies  
7 (listed in Supplementary Table 4). Quantitative analyses of glial fibrillary acidic protein  
8 (GFAP) -positive astrocytes, oligodendrocyte transcription factor (Olig2) -positive  
9 oligodendrocyte lineage cells, and myelin basic protein (Mbp) -positive mature  
10 oligodendrocytes were performed in the bilateral paramedian corpus callosum using  
11 Image J.

12

13 **Western blot**

14

15 Western blot analysis was performed as previously described (28). Briefly, the dorsal  
16 half of the brain at 0–0.5 mm anterior to bregma was homogenized in  
17 radio-immunoprecipitation assay buffer, followed by sonication for 5 min with a 30-sec  
18 interval and centrifugation at 14000 rpm for 5 min at  $4^{\circ}\text{C}$ . The supernatant was boiled in  
19 sample buffer (1% (w/v) Sodium dodecyl sulfate (SDS), 12.5% (w/v) glycerol, 0.005%  
20 (w/v) bromophenol blue, and 2.5% (v/v) 2-mercaptoethanol in 25 mM Tris-HCl, pH  
21 6.8). Samples were separated onto 10% (w/v) gels for SDS-PAGE or 4–12% (w/v) gels  
22 for NuPAGE (NP032330X, Invitrogen), followed by transfer to polyvinylidene  
23 difluoride membranes (Millipore, MA, USA). The membranes were then incubated  
24 overnight at  $4^{\circ}\text{C}$  with primary antibodies (listed in Supplementary Table 5) followed by



1 the appropriate horseradish peroxidase-conjugated secondary antibodies for 1 h at room  
2 temperature. Immunoreactive bands were detected with chemiluminescence assay kits  
3 (02230, Nacalai tesque) and Amersham Imager 600 (GE Healthcare, Buckinghamshire,  
4 UK).

5

## 6 **Statistical analysis**

7

8 Statistical analysis was performed using the R statistical package ([www.r-project.org](http://www.r-project.org)).  
9 Statistical significance was evaluated using two-tailed paired Student's t-test, the  
10 Wilcoxon rank-sum test, or one-way ANOVA followed by the Bonferroni post-hoc test.  
11 Pearson correlation analysis was performed to observe a possible correlation. For all  
12 analyses, the level of statistical significance was set at  $**P < 0.01$  or  $*P < 0.05$ .

13

## 14 **Results**

15

### 16 **Myelin loss in SVD and AD compared with controls**

17

18 Luxol fast blue staining (Figure 1B) and MBP immunohistochemical staining (Figure  
19 1C) represented severe myelin attenuation in the SVD group. The myelin index was  
20 significantly different between the SVD group and the other two groups as follows:  
21 controls (80.9) > AD (71.5) > SVD (56.3) (Figure 1D), indicating that myelin loss was  
22 greatest in the SVD group. Age did not correlate with myelin index ( $r = -0.329$ ,  $P =$   
23  $0.170$ , data not shown). The percent area of MBP immunoreactivity also decreased in  
24 the SVD group (Figure 1E).

1  
2  
3  
4  
5  
6  
7  
8  
9  
10  
11  
12  
13  
14  
15  
16  
17  
18  
19  
20  
21  
22  
23  
24

## **Capillary bed density**

Capillary bed density was determined by immunohistochemistry using antibody specific to COL4A1, a major constituent of the basement membrane (Figure 1F). Quantitative analysis showed that the percentage of COL4A1 density was not different in the white matter or cortex between the three groups (white matter,  $P = 0.095$ ; cortex,  $P = 0.095$ ) (Figure 1G).

## **Pericyte density in the postmortem human brain**

Pericyte density was assessed by two different markers: ACTA2 and platelet-derived growth factor receptor beta (PDGFRB). The percentage of ACTA2 and PDGFRB expression, respectively, were divided by the percentage of COL4A1 stained area to correct for vascular density.

The ACTA2 immunoreactivity was not different in the white matter and cortex between the three groups (white matter,  $P = 0.123$ ; cortex,  $P = 0.220$ ) (Figure 2A and B). Conversely, the percentage of PDGFRB expression was significantly increased in white matter of the SVD group compared with the other two groups (Figure 2C and D). There was a significant inverse correlation between the percentage of PDGFRB/COL4A1 expression in the white matter and myelin index in all 19 cases combined ( $r = -0.568$ ,  $*P = 0.013$ ) (Figure 2E).

## **BMP4 expression in PDGFRB-positive pericytes of damaged white matter in the**

1 **postmortem human brain**

2

3 BMP4 was strongly expressed in abluminal surface of capillaries and tunica media of  
4 arterioles, and mildly expressed in macrophages, and activated astrocytes in the white  
5 matter of SVD brains. Triple immunofluorescence studies revealed abundant BMP4  
6 expression in PDGFRB- and ACTA2 -positive pericytes in the white matter of SVD  
7 cases. However, in control or AD brains, BMP4 expression was weak (Figure 3A).

8 Similar to the percentage of PDGFRB/COL4A1 expression, the percentage of  
9 BMP4/COL4A1 expression was significantly increased in the white matter of SVD  
10 cases but was not different in the cortex between the three groups (Figure 3B). BMP4  
11 expression negatively correlated with the myelin index ( $r = -0.549$ ,  $*P = 0.015$ ) (Figure  
12 3C) in all 19 cases combined. Fluorescence intensity and percentage of BMP4-positive  
13 area in PDGFRB- and ACTA2-positive cells were increased in SVD cases (Figure 3D to  
14 3G), suggesting BMP4 expression was increased in pericytes. BMP4 expression was  
15 also observed in activated astrocytes and macrophages in SVD, but not control or AD,  
16 cases (data not shown).

17

18 **Other TGF $\beta$  superfamily members (TGFB1, BMP2, BMP6, BMP7, and BMP9)**

19

20 Macrophages and activated astrocytes within the vicinity of microinfarcts were  
21 immunoreactive to all six TGF superfamily members. BMP2 was highly expressed in  
22 the endothelial cells of arterioles, venules, and capillaries in all three groups. BMP7 and  
23 TGFB1 were slightly expressed in the tunica media of arterioles and capillaries. BMP6  
24 and BMP9 were not expressed in blood vessels (Supplementary Figure 1).

1

## 2 **Oligodendrocyte precursor cells and astrocytes in the postmortem human brain**

3

4 PDGFRA-positive OPCs were found in the subventricular zone (SVZ), and cellular  
5 processes of some OPCs were found around arterioles, venules, and capillaries (Figure  
6 3H, Supplementary Figure 2). The number of brain interstitial OPCs was measured in  
7 the SVZ of all cases and found to be increased relative to white matter attenuation, as  
8 previously described (33). However, when the SVD cases were divided into two groups  
9 by the cut-off point of 0.31 for BMP4/COL4A1, the higher BMP4/COL4A1 group  
10 (SVD 2, n = 4) tended to have a smaller number of OPCs than the lower  
11 BMP4/COL4A1 group (SVD 1, n = 3) (Figure 3I). The GFAP-positive astrocytes were  
12 increased in the white matter of SVD cases (Figure 3J).

13

## 14 **BMP4 expression in cultured pericytes under oxygen-glucose deprivation**

15

16 To confirm whether BMP4 is increased in pericytes under chronic hypoperfusion, we  
17 analyzed *Bmp4* mRNA expression in cultured pericytes under continuous OGD. The  
18 mouse brain microvascular pericyte cell line expressed both *Pdgfrb* and *Acta2* (Figure  
19 4A). *Bmp4* mRNA expression exhibited a time-dependent increase under continuous  
20 OGD for 3 days (Figure 4B). *Pdgfrb*, but not *Acta2*, mRNA expression increased under  
21 OGD (Figure 4C and 4D). Expression of each mRNA sample was normalized to  
22 hypoxanthine-guanine phosphoribosyltransferase expression (*Hprt*) expression, which  
23 did not fluctuate under continuous OGD.

24

### 1 **Effects of BMP4 on pericyte proliferation and *Pdgfrb/Acta2* mRNA expression**

2  
3 The WST-8 assay showed that high-dose BMP4 induced pericyte proliferation (Figure  
4 4E). BMP4 also increased *Pdgfrb* (Figure 4F) and *Acta2* (Figure 4G) mRNA expression  
5 levels.

### 6 7 **Effects of BMP4 on endothelial cell proliferation and tube formation**

8  
9 Endothelial cell proliferation in response to BMP4 treatment was assessed by  
10 immunocytochemistry (Figure 4H) and WST-8 assay (Figure 4I). Endothelial cell  
11 proliferation and tube formation (Figure 4J and 4K) were facilitated in a dose-dependent  
12 manner by BMP4, but were blocked by the BMP4 antagonist, noggin.

### 13 14 **Effects of BMP4 on oligodendrocyte precursor cells**

15  
16 In the OPC proliferation assay, treatment of BMP4 converted OPCs into astrocyte-like  
17 cells, with thick and long processes (Figure 5A and Supplementary Movie 1).  
18 Immunocytochemistry showed that BMP4 treatment decreased *Pdgfra* (OPC marker)  
19 immunoreactivities and increased *Gfap* (astrocyte maker) (Figure 5B). RT-PCR also  
20 showed that BMP4 decreased *Pdgfra* mRNA levels, and significantly increased *Gfap*  
21 mRNA levels in a dose-dependent manner; noggin blocked the conversion (Figure 5C  
22 and 5D). Treatment with noggin alone increased *Pdgfra* mRNA levels in OPCs due to  
23 inhibition of endogenous BMP4 (Figure 5C)

24 The effects of BMP4 on OPCs were also observed in the OPC differentiation assay. In

1 the differentiation media, primary OPCs differentiated into mature oligodendrocytes,  
2 whereas BMP4 treatment induced astrocyte-like cells (Supplementary Figure 3A and  
3 Supplementary Movie 2). BMP4 treatment decreased Mbp (oligodendrocyte marker)  
4 and increased Gfap in a dose-dependent manner; noggin also blocked the conversion  
5 (Supplementary Figure 3B to 3D).

6

### 7 **Bmp4 expression and effect of noggin in the mouse brain under chronic** 8 **hypoperfusion**

9

10 Adult mice subjected to BCAS and noggin cICV (or ACSF only) treatment were  
11 analyzed by immunohistochemistry and western blot (Figure 6A and 6H). The  
12 inhibitory effect of noggin on BMP signaling was confirmed by a reduction of  
13 phosphorylated Smad immunoreactivity (data not shown).

14 Bmp4 was expressed in the Acta2/Pdgfrb double-positive pericytes in capillaries of  
15 28-days-BCAS mouse brains (Figure 6B). Western blot showed significantly increased  
16 expression of Bmp4 precursor (Figure 6C and 6D, and Supplementary Figure 4A) and  
17 Pdgfrb (Figure 6E and 6F, and Supplementary Figure 4B), but not Acta2 (Figure 6E and  
18 6G, and Supplementary Figure 4C) after BCAS, compared with sham controls. The  
19 Bmp4 precursor (41) was detected by both C-terminal (ab39973, Abcam, Cambridge,  
20 UK) and N-terminal (MAB1049, Millipore, and sc-393329, SantaCruz, Dallas, TX,  
21 USA) domain antibodies (data not shown). The expressions of western blot sample were  
22 normalized to tubulin gamma 1 (Tubg1) expression, which did not fluctuate under  
23 hypoperfusion.

24 The percent area of Gfap expression increased after BCAS, which was suppressed by

1    noggin cICV (Figure 6I and 6J). The percent area of Olig2 expression was decreased by  
2    BCAS, which was ameliorated by noggin cICV at a dosage of 1000 ng/day (Figure 6I  
3    and 6K). Western blot also showed significantly increased Gfap expressions in the  
4    BCAS mice, which was suppressed by noggin cICV (both 500 ng/day and 1000 ng/day)  
5    (Figure 6L and 6M, and supplementary Figure 4D). Olig2 expression was decreased by  
6    BCAS, which was ameliorated by a high dose of noggin cICV (1000 ng/day) (Figure 6L  
7    and 6N, and supplementary Figure 4E). Each band of Gfap and Olig2 was normalized  
8    with non-specific band stained with ponceau S staining (Figure 6L and Supplementary  
9    Figure 4F). To assess the effect of BMP4 on mature oligodendrocytes, the percent area  
10   of Mbp expression was quantitated. The percent area of Mbp was decreased by BCAS,  
11   which was ameliorated by noggin cICV at a dosage of 1000 ng/day (Figure 6O and 6P).

12

### 13    **Discussion**

14

15   We previously reported that myelin loss evolved in parallel with shrunken  
16   oligodendrocytes in SVD compared to AD (20). Another study revealed that spongiosis,  
17   arteriolosclerosis, état criblé, and myelin loss were more severe in the SVD cases than  
18   the AD cases (13), suggesting different etiologies underlie the white matter attenuation  
19   between SVD and AD. In this study, we clarified one of the causative factors underlying  
20   the different aspects of white matter changes: namely, BMP4 generated from pericytes.  
21   We analyzed expressions of six TGFB superfamily members in the brains of SVD, AD,  
22   and age-matched controls, and found BMP4 was distinctly expressed in pericytes of the  
23   white matter. BMP4 expression was significantly upregulated in the SVD group, and  
24   was negatively correlated with myelin density. Consistent with these findings, long-term

1 OGD in cultured pericytes and *in vivo* chronic hypoperfusion induced BMP4  
2 upregulation. Given that chronic hypoperfusion during late embryonic stages (36) and  
3 neonatal stages (12) increases BMP4 expression and impairs differentiation of OPCs,  
4 chronic hypoperfusion may also upregulate BMP4 in the elderly. Recent evidence  
5 suggests that Tgfb upregulation contributes to cerebrovascular dysfunction in mice (34),  
6 which ascertains CARASIL pathogenesis in humans through hereditary loss of *HtrAI*  
7 (18). Therefore, these results suggest upregulation of the TGF $\beta$  superfamily members is  
8 a shared mechanism in the pathogenesis of ischemic cerebrovascular disorders,  
9 regardless of whether it is sporadic or hereditary.

10 Previous studies have shown that Bmps, including Bmp2, 4, 6 and 7, are upregulated in  
11 a variety of CNS injury and demyelinating disease animal models (14, 45). In this study,  
12 expression of all six TGF $\beta$  superfamily members was also observed in macrophages  
13 and activated astrocytes within the vicinity of microinfarcts in the SVD group. However,  
14 in demyelinated but not infarcted areas, of the SVD group, BMP4 was almost  
15 exclusively expressed in pericytes.

16 The density of PDGFR $\beta$ -positive pericytes in the white matter correlated with myelin  
17 attenuation. In previous studies, PDGFR $\beta$  immunostaining was used to assess  
18 microvasculature, showing a reduction of PDGFR $\beta$ -positive pericytes and a breakdown  
19 of the blood-brain barrier in vascular cognitive impairment and some neurodegenerative  
20 diseases, including, AD, and ALS (46, 51, 55, 56, 59). However, a recent study showed  
21 increased expression of PDGFR $\beta$  immunoreactive pericytes in cerebral microvessels in  
22 CADASIL (cerebral autosomal dominant arteriopathy with subcortical infarcts and  
23 leukoencephalopathy) compared with similar age controls (11). It has also been  
24 suggested that *Pdgfrb* mRNA is upregulated in pericytes in the infarcted area (37), and



1 *Pdgfrb*-positive pericytes migrate into the peri-infarct area after stroke, contributing to  
2 angiogenesis and vascular remodeling (25). In the current study, *Pdgfrb* expression was  
3 also upregulated by chronic hypoperfusion in the BCAS mice. Given that the PDGFRB  
4 is important for proliferation and migration of pericytes (55), PDGFRB may be  
5 increased in pericytes at a certain point, as compensation for hypoperfusion.

6 Unlike PDGFRB, ACTA2 expression was not different between the three groups. In  
7 terms of tumor angiogenesis, *Acta2* served as a mature pericyte marker whereas *Pdgfrb*  
8 served as a marker for progenitor perivascular cells with the ability to differentiate into  
9 pericytes and regulate vessel stability and vascular survival (50). Therefore, the  
10 differences in PDGFRB and ACTA2 expression may be the result of different stages of  
11 pericyte maturation; PDGFRB-positive pericytes in the white matter are immature  
12 pericytes during angiogenesis following chronic hypoperfusion, and  
13 PDGFRB-negative/ACTA2-positive pericytes are mature pericytes in relatively intact  
14 white matter. Because BMP4 treatment facilitated pericyte proliferation and *Pdgfrb*  
15 mRNA expression, an increase in PDGFRB-positive pericytes in the SVD group might  
16 be induced by BMP4 in response to chronic hypoperfusion. BMP4 also facilitated  
17 proliferation and tube formation of endothelial cells, which is another key factor for  
18 maintenance of vascular integrity. These results suggest that BMP4 induces inherent  
19 compensatory angiogenesis against chronic hypoperfusion. Despite the putative  
20 compensatory responses, COL4A1-positive vessel density was not significantly  
21 different in SVD compared with AD or disease control patients in the cerebral cortex  
22 and white matter, suggesting that angiogenesis was not sufficient or compensatory  
23 enough to recruit blood vessels and mitigate cerebral hypoperfusion in SVD patients.  
24 Because time-specific induction of BMP4 and PDGFRB is necessary for successful

1 angiogenesis, long-lasting hypoperfusion in the aged brain may block appropriate  
2 angiogenesis to restore regional blood flow (52).

3 With regard to myelination, BMP4 overexpression may not be preferable. BMP4  
4 treatment has been shown to induce differentiation of oligodendroglial-astroglial  
5 progenitor cells into astrocytes (17, 27). Our results also showed that BMP4 strongly  
6 suppressed maturation of primary OPCs and converted OPCs into astrocytes in  
7 differentiation media. Compared with 1.2- to 2-fold changes in angiogenesis, the degree  
8 of inducing astrogliogenesis and suppressing oligodendrogenesis was exponential.  
9 Furthermore, even when the OPCs were cultured in proliferation media which should  
10 maintain an OPC state, BMP4 treatment decreased *Pdgfra* mRNA expression in a  
11 dose-dependent manner. This finding was inconsistent with other studies that  
12 demonstrated no effect (16, 57) or even a positive effect (43) of BMP4 on OPC  
13 proliferation. However, recent studies have suggested that the effects of BMP4 on stem  
14 cell proliferation are dose-dependent; low dose BMP4 increases proliferation, but high  
15 dose BMP4 decreases proliferation of mesenchymal stem cells (53) or primordial germ  
16 cells (31). Considering that OPC proliferation is also affected by many factors, BMP4  
17 may have dose-dependent and opposite effects on OPC proliferation. Consistent with  
18 the results of cell culture, the number of OPCs in SVZ is decreased with higher BMP4  
19 expression of SVD cases with severe astrogliosis. BCAS mice also showed astrogliosis  
20 and hypomyelination as shown previously (48). As noggin, a receptor antagonist of  
21 BMP4, suppressed astrogliogenesis and induced oligodendrogenesis *in vitro*, both high  
22 and low doses of noggin cICV decreased the number of astrocytes and high dose of  
23 noggin cICV increased the number of oligodendrocytes.

24 The close relationship between BMP4 and myelin attenuation is also supported by

1 recent studies (3, 15, 26, 43). These data strongly suggest that BMPs are involved in  
2 oligovascular pathologies in the brain. Considering a potential anatomical and  
3 functional interaction between pericytes and OPCs in the capillary of cerebral white  
4 matter (30), the pericyte-induced BMP4 might directly affect OPC lineage. Because  
5 many factors should be expressed in a coordinated manner after cerebral hypoperfusion,  
6 time-specific control of BMP expression should be further investigated to protect  
7 oligovascular units in ischemic demyelinating diseases.

8 The main limitation of this study was the lack of clinical and neuropsychometric  
9 information on the postmortem brains used. This meant that we could not directly relate  
10 our pathological findings to antemortem hypoperfusive and cognitive status. In addition,  
11 the lack of comparison of the SVD cases with controls without neurodegenerative  
12 pathologies was another limitation considering that PDGFRB positive pericytes may  
13 also degenerate in some neurodegenerative diseases (46, 55, 56, 59). The third  
14 limitation is that a histopathological study using postmortem human brains does not  
15 always uncover the entire cell process that occurs in the ageing human brain. Although  
16 the process was at least partially modeled by both cultured pericytes under OGD and  
17 mice subjected to BCAS, future studies should focus on examining dynamic changes of  
18 pericyte disruption and BMP4 values in the disease course of SVD using neuroimaging  
19 and biomarkers.

20 In summary, our study suggests that during chronic hypoperfusion akin to that in SVD,  
21 BMP4 is generated in pericytes predominantly in the white matter, providing putative  
22 compensatory angiogenesis. However, BMP4 also aggravates white matter damage by  
23 inducing astroglialogenesis at the expense of OPC proliferation and maturation. Based on  
24 our observations, we propose a putative scheme how these cellular processes could

1 occur (Figure 7). This may explain why white matter is particularly vulnerable to  
2 chronic hypoperfusion.

#### 3 4 **Acknowledgements**

5  
6 We thank Dr. Masato Maesako, Dr. Norihito Uemura, and Dr. Yusuke Hatanaka for  
7 insightful discussions and technical advice; we thank Ryotaro Tamano and Rie Hikawa  
8 for technical assistance, and Dr. Ahmad Khundakar for editing the manuscript and  
9 giving insightful suggestions. We gratefully acknowledge grant support from the  
10 Ministry of Health, Labour, and Welfare (M.I., No. 0605-1), the Ministry of Education,  
11 Culture, Sports, Science, and Technology (M.I., Scientific Research (B), No.  
12 15H04271), and the Integrated Neurotechnologies for Disease Studies (Brain/MINDS)  
13 from Japan Agency for Medical Research and Development, AMED (R.T., No.  
14 16dm0207020h0003). RNK's work is supported by grants from the UK Medical  
15 Research Council (MRC, G0500247), Dunhill Medical Trust UK, and Alzheimer's  
16 Research UK.

#### 17 18 **Author contributions**

19  
20 M.U. study design, acquisition and analysis of data, and drafting the manuscript and  
21 figures; M.I. study conception and design, handling funding, and supervising portions of  
22 the study; T.M. design of the study, and supervising and making critical revision of the  
23 manuscript for important intellectual content; T.N. data acquisition and analysis, and  
24 supervising and making critical revision of the manuscript for important intellectual

1 content; S.K. data acquisition and analysis; K.U., R.N.K., and A.K. supervising and  
2 making critical revision of the manuscript for important intellectual content.; R.T.  
3 handling funding, supervising and making critical revision of the manuscript for  
4 important intellectual content.

5

## 6 **Figure Legends**

7

8 **Figure 1. Degree of myelin loss and capillary bed density in the frontal lobes of**  
9 **post-mortem human brain samples.** (A) A procedure for calculating myelin index.  
10 The median gray level of each quartile (14.5, 46.0, 78.5, and 111.0) is multiplied by  
11 percent area in each quartile (29.27%, 69.28%, 1.44%, and 0.01%), and summed up to  
12 be 37.25 as the myelin index for the representative image of LFB staining. *Bar* indicates  
13 5 mm. (B) Representative images of LFB staining in control, AD, and SVD cases. *Bar*  
14 indicates 5 mm. (C) Representative images of MBP staining (myelin) in control, AD,  
15 and SVD cases. *Bar* indicates 400  $\mu$ m. *Black triangles* indicate cortex. *Asterisks* mean  
16 U-fiber. (D) Myelin index calculated from each LFB staining of all three groups.  
17 Differences are significant between any two groups, except between control and AD:  
18 control vs. AD,  $P = 0.226$ ; control vs. SVD,  $**P = 0.001$ ; AD vs. SVD,  $*P = 0.027$ . (E)  
19 The percentage of MBP in the WM in all three groups. Differences are significant  
20 between any two groups, except between AD and SVD: control vs. AD,  $*P = 0.027$ ;  
21 control vs. SVD,  $**P = 0.001$ ; AD vs. SVD,  $P = 0.224$ . (F) Representative images of  
22 COL4A1 staining (basement membrane marker) in control, AD, and SVD cases. *Bar*  
23 indicates 100  $\mu$ m. (G) The percentage of COL4A1 in the WM and cortex in all three  
24 groups. Differences are not significant in the WM ( $P = 0.095$ ) and cortex ( $P = 0.095$ ).

1 *Vertical bars* represent mean  $\pm$  SEM. Abbreviations are as follows: AD, Alzheimer's  
2 disease; Cont, control; MBP, myelin basic protein; LFB, Luxol fast blue; SVD, small  
3 vessel disease; WM, white matter.

4

5 **Figure 2. Pericyte density as assessed by ACTA2 and PDGFRB labeling in the**

6 **post-mortem human brain samples.** (A) Representative images of ACTA2 staining in

7 control, AD, and SVD cases. Insets show ACTA2-positive pericytes. *Bars* indicate 100

8  $\mu\text{m}$  and 10  $\mu\text{m}$  (insets). (B) The percentage of ACTA2 in the WM and cortex in all three

9 groups. Differences are not significant in the WM ( $P = 0.123$ ) and cortex ( $P = 0.220$ ).

10 (C) Representative images of PDGFRB staining in control, AD, and SVD cases. Insets

11 show PDGFRB-positive pericytes. *Bars* indicate 100  $\mu\text{m}$  and 10  $\mu\text{m}$  (insets). (D) The

12 percentage of PDGFRB in the WM and cortex in all three groups. Differences are

13 significant between control and SVD in the WM: control vs. AD,  $P = 0.955$ ; control vs.

14 SVD,  $*P = 0.046$ ; AD vs. SVD,  $P = 0.081$ . Differences are not significant in the cortex ( $P$

15  $= 0.464$ ). (E) An inverse correlation between the percentage of PDGFRB and the myelin

16 index all 19 cases combined ( $r = -0.568$ ,  $*P = 0.013$ ). *Vertical bars* represent mean  $\pm$

17 SEM. Abbreviations are as follows: AD, Alzheimer's disease; Cont, control; SVD, small

18 vessel disease; WM, white matter.

19

20 **Figure 3. Pericyte BMP4 expression in damaged white matter in the post-mortem**

21 **human brain samples.** (A) Representative triple-immunofluorescent images for BMP4,

22 PDGFRB, and ACTA2, and their merged images in the WM of all three groups. Insets

23 show enlarged pericytes. *Bars* indicate 100  $\mu\text{m}$  and 10  $\mu\text{m}$  (insets). (B) The percentage of

24 BMP4 expression in all three groups. Differences are significant between any two groups,

1 except between control and AD in the WM: control vs. AD,  $P = 0.804$ ; control vs. SVD,  
2  $**P = 0.003$ ; AD vs. SVD,  $*P = 0.012$ . Differences are not significant in the cortex ( $P =$   
3  $0.659$ ). (C) An inverse correlation between the percentage of BMP4 expression and the  
4 myelin index in all 19 cases combined ( $r = -0.549$ ,  $*P = 0.015$ ). (D) The percent area of  
5 BMP4 expression in PDGFRB-positive cells in the WM of all three groups. Differences  
6 are significant between any two groups, except between control and AD: control vs. AD,  
7  $P = 0.593$ ; control vs. SVD,  $**P = 0.001$ ; AD vs. SVD,  $*P = 0.011$ . (E) The mean  
8 intensity of BMP4 in PDGFRB-positive cells in the WM of all three groups. Differences  
9 are significant between any two groups: control vs. AD,  $**P < 0.001$ ; control vs. SVD,  
10  $**P < 0.001$ ; AD vs. SVD,  $*P = 0.017$ . (F) The percent area of BMP4 expression in  
11 ACTA2-positive cells in the WM of all three groups. Differences are significant between  
12 any two groups, except between control and AD: control vs. AD,  $P = 0.079$ ; control vs.  
13 SVD,  $**P < 0.001$ ; AD vs. SVD,  $**P < 0.001$ . (G) The mean intensity of BMP4 in  
14 ACTA2-positive cells in the WM of all three groups. Differences are significant between  
15 any two groups: control vs. AD,  $**P < 0.001$ ; control vs. SVD,  $**P < 0.001$ ; AD vs. SVD,  
16  $*P = 0.018$ . (H) Representative images of PDGFRA expression in the interstitium of the  
17 SVZ in the cases of control, AD, and SVD of post-mortem human brain samples.  
18 According to expression levels of BMP4 (BMP4-to-COL4A1 ratio), the SVD cases are  
19 further classified into subgroup: a lower BMP-4 expressing group (SVD 1) and a higher  
20 one (SVD 2) with the cut-off ratio of 0.31. Insets show enlarged images of OPCs. *Bars*  
21 indicate 50  $\mu\text{m}$  and 10  $\mu\text{m}$  (insets). (I) The number of OPCs in all 4 groups. SVD 2  
22 group shows smaller number of OPCs compared with SVD 1 group. (J) Representative  
23 images of GFAP expression in the WM of post-mortem human brain samples. The WM  
24 of SVD shows severe astrogliosis with high GFAP expression. *Bar* indicates 50  $\mu\text{m}$ .

1 Vertical bars represent mean  $\pm$  SEM. Abbreviations are as follows: AD, Alzheimer's  
2 disease; Cont, control; SVD, small vessel disease; WM, white matter.

3

4 **Figure 4. Effects of BMP4 expression on cultured endothelial cells and pericytes.**

5 (A) Representative images of mouse pericyte cell line. The cells express *Pdgfrb* and  
6 *Acta2*, both established pericyte markers. *Bar* indicates 50  $\mu$ m. (B–D) Relative mRNA  
7 levels of *Bmp4* (B), *Pdgfrb* (C), and *Acta2* (D) in cultured pericytes under OGD. *Bmp4*  
8 mRNA levels show a time-dependent increase with continuous OGD for 3 days ( $*P =$   
9 0.024 for Day 1 and  $**P < 0.001$  for Days 2 and 3). *Pdgfrb* mRNA levels are increased  
10 ( $**P < 0.001$  for Days 1, 2 and 3), but *Acta2* mRNA levels are decreased ( $**P < 0.001$   
11 for Days 1, 2 and 3) by OGD. The expression of each mRNA sample is normalized to  
12 *Hprt* expression, which does not fluctuate under continuous OGD. (E) Relative viability  
13 of pericytes as assessed by WST-8 assay. High-dose BMP4 increases pericyte viability  
14 ( $**P < 0.001$  for 50 ng/ml), which is blocked by noggin ( $**P = 0.009$ ). (F, G) Relative  
15 mRNA levels of *Pdgfrb* and *Acta2* in cultured pericytes after BMP4 administration.  
16 BMP4 increases *Pdgfrb* mRNA levels in a dose-dependent manner ( $**P = 0.001$  for 10  
17 ng/ml and  $**P < 0.001$  for 50 ng/ml), which is blocked by noggin ( $**P = 0.009$ ) (F).  
18 BMP4 increases *Acta2* mRNA levels ( $**P < 0.001$  for 1, 10 and 50 ng/ml), which is  
19 blocked by noggin ( $**P = 0.002$ ) (G). (H) Representative images of PECAM1-positive  
20 endothelial cells after additions of BMP4 with or without noggin. *Bar* indicates 50  $\mu$ m.  
21 (I) Relative viability of endothelial cells as assessed by WST-8 assay. BMP4 increases  
22 viability of endothelial cells in a dose-dependent manner ( $**P < 0.001$  for 1, 10 and 50  
23 ng/ml), which is blocked by noggin ( $**P < 0.001$ ). (J) Representative images of  
24 endothelial cell tube formation after BMP4 additions with or without noggin. *Bar*



1 indicates 100  $\mu\text{m}$ . (K) BMP4 facilitates tube formation of endothelial cells (\*\* $P = 0.008$   
2 for 50 ng/ml), which is blocked by noggin (\*\* $P < 0.001$ ). *Vertical bars* represent mean  $\pm$   
3 SD. Abbreviations are as follows: ECs, endothelial cells; Gapdh,  
4 glyceraldehyde-3-phosphate dehydrogenase; Hprt, hypoxanthine-guanine  
5 phosphoribosyltransferase expression; OGD, oxygen-glucose deprivation; PECAM1,  
6 platelet and endothelial cell adhesion molecule 1, also known as CD31.

7

8 **Figure 5. Effects of BMP4 on cultured oligodendrocyte precursor cells.** (A)  
9 Time-lapse images of primary OPCs in proliferation media with or without BMP4.  
10 Insets show enlarged images. *Bars* indicate 100  $\mu\text{m}$  and 50  $\mu\text{m}$  (insets). (B)  
11 Representative triple-immunofluorescent images for *Pdgfra* and *Gfap*, and their merged  
12 images with DAPI for nuclear staining. Insets show enlarged images. *Bars* indicate 50  
13  $\mu\text{m}$  and 10  $\mu\text{m}$  (insets). (C, D) Relative mRNA levels of *Pdgfra* and *Gfap* in the  
14 proliferation assay. (C) BMP4 decreases *Pdgfra* mRNA levels in a dose-dependent  
15 manner ( $P = 0.062$  for 1 ng/ml and \*\* $P < 0.001$  for 10 ng/ml), which is blocked by  
16 noggin (\*\* $P = 0.001$ ). Treatment with noggin alone increases *Pdgfra* mRNA levels ( $*P$   
17 = 0.015). (D) BMP4 significantly increases *Gfap* mRNA expression in a dose-dependent  
18 manner (\*\* $P = 0.004$  for 1 ng/ml and \*\* $P < 0.001$  for 1 and 10 ng/ml), which is blocked  
19 by noggin (\*\* $P < 0.001$ ). *Vertical bars* represent mean  $\pm$  SD. Abbreviations are as  
20 follows: Cont, control; Gapdh, glyceraldehyde-3-phosphate dehydrogenase.

21

22 **Figure 6. BMP4 expression and effect of noggin in the mouse brain after chronic**  
23 **hypoperfusion.** (A) Experimental design of the first trial. Adult mice subjected to  
24 BCAS are analyzed by immunohistochemistry and western blot. (B) Representative

1 triple-immunofluorescent images for Bmp4, Pdgfrb, and Acta2, and their merged  
2 images with DAPI for nuclear staining. *Bars* indicate 10  $\mu\text{m}$ . (C–G) Western blot shows  
3 significantly increased Bmp4 precursor (C, D) and Pdgfrb (E, F) levels after BCAS  
4 (\*\* $P = 0.002$  for Bmp4 precursor and \*\* $P = 0.004$  for Pdgfrb), with not significantly  
5 changes in Acta2 levels ( $P = 0.660$ ) (E, G). (H) Experimental design of the second trial.  
6 Adult mice subjected to BCAS receive noggin (500 ng/day or 1000 ng/day) in ACSF or  
7 ACSF only through cICV two days prior to BCAS, are euthanized and their brains  
8 analyzed by immunohistochemistry and western blot. (I) Representative  
9 immunofluorescent images of Gfap and Olig2 with DAPI (the leftmost images) and  
10 their enlarged images (three right images). *Bars* indicate 500  $\mu\text{m}$  (left) and 100  $\mu\text{m}$   
11 (right). (J) Semiquantitative analysis of immunofluorescent images shows that BCAS  
12 significantly increases GFAP-positive cells (\*\* $P = 0.004$ ), which is strongly suppressed  
13 by noggin cICV (\*\* $P < 0.001$  for both 500 ng/day and 1000 ng/day). (K)  
14 Semiquantitative analysis of immunofluorescent images shows BCAS significantly  
15 decreases Olig2-positive cells (\*\* $P < 0.001$ ), which is significantly ameliorated by high  
16 dose of noggin cICV ( $P = 0.771$  for 500 ng/day and \* $P = 0.026$  for 1000 ng/day). (L,  
17 M) Western blot shows significantly increased Gfap levels after BCAS (\*\* $P < 0.001$  for  
18 Sham vs. BCAS + ACSF), which is suppressed by noggin cICV (\*\* $P < 0.001$  for BCAS  
19 + ACSF vs. BCAS + noggin 500 and 1000 ng/day) (L, N). Western blot shows  
20 significantly decreased Olig2 levels after BCAS (\* $P = 0.030$  for Sham vs. BCAS +  
21 ACSF), which is ameliorated by a high dose of noggin cICV ( $P = 0.698$  for BCAS +  
22 ACSF vs. BCAS + noggin 500 ng/day; and \* $P = 0.042$  for BCAS + ACSF vs. BCAS +  
23 noggin 1000 ng/day). (O, P) Semiquantitative analysis of immunofluorescent images  
24 shows that BCAS significantly decreases Mbp (\*\* $P = 0.001$ ), which is significantly

1 ameliorated by high dose of noggin cICV ( $P = 0.169$  for 500 ng/day and  $*P = 0.034$  for  
2 1000 ng/day). *Bars* indicate 100  $\mu\text{m}$ . *Vertical bars* represent mean  $\pm$  SEM.  
3 Abbreviations are as follows: B, BCAS; cICV, continuous intracerebroventricular  
4 infusion; IHC, immunohistochemistry; N500, noggin 500 ng/day; N1000, noggin 1000  
5 ng/day; S, Sham operation; Tubj1, tubulin gamma 1, also known as gamma tubulin; WB,  
6 western blot.

7

8 **Figure 7. Putative scheme for BMP4 effect on multiple cell lineages after chronic**  
9 **ischemia.** BMP4 generated from pericytes after hypoperfusion may promote  
10 compensatory angiogenesis by significantly increasing production of endothelial cells  
11 and pericytes. However, BMP4 expression may also induce astroglialogenesis at the  
12 expense of OPC proliferation and maturation, thereby aggravating white matter damage.  
13 Noggin has the potential to suppress BMP4-induced astroglialogenesis and rescue  
14 oligodendrogenesis.

## 1   **References**

2

3   1.       Akiguchi I, Tomimoto H, Suenaga T, Wakita H, Budka H (1998) Blood-brain  
4   barrier dysfunction in Binswanger's disease; an immunohistochemical study. *Acta*  
5   *Neuropathol.*95(1):78-84.

6   2.       American Psychiatric, Association (1994) Diagnostic and statistical manual of  
7   mental disorders, 4th edn. American Psychiatric Press, Washington, DC.

8   3.       Ara J, See J, Mamontov P, Hahn A, Bannerman P, Pleasure D, Grinspan JB  
9   (2008) Bone morphogenetic proteins 4, 6, and 7 are up-regulated in mouse spinal cord  
10   during experimental autoimmune encephalomyelitis. *J Neurosci Res.*86(1):125-35.

11   4.       Back SA, Kroenke CD, Sherman LS, Lawrence G, Gong X, Taber EN, Sonnen  
12   JA, Larson EB, Montine TJ (2011) White matter lesions defined by diffusion tensor  
13   imaging in older adults. *Ann Neurol.*70(3):465-76.

14   5.       Bennett DA, Wilson RS, Gilley DW, Fox JH (1990) Clinical diagnosis of  
15   Binswanger's disease. *J Neurol Neurosurg Psychiatry.*53(11):961-5.

16   6.       Braak H, Alafuzoff I, Arzberger T, Kretschmar H, Del Tredici K (2006)  
17   Staging of Alzheimer disease-associated neurofibrillary pathology using paraffin  
18   sections and immunocytochemistry. *Acta Neuropathol.*112(4):389-404.

19   7.       Braak H, Braak E (1991) Neuropathological staging of Alzheimer-related  
20   changes. *Acta Neuropathol.*82(4):239-59.

21   8.       Chen Y, Balasubramanian V, Peng J, Hurlock EC, Tallquist M, Li J, Lu QR  
22   (2007) Isolation and culture of rat and mouse oligodendrocyte precursor cells. *Nat*  
23   *Protoc.*2(5):1044-51.

24   9.       Choi JC (2015) Genetics of cerebral small vessel disease. *J Stroke.*17(1):7-16.

- 1 10. Chui HC, Zheng L, Reed BR, Vinters HV, Mack WJ (2012) Vascular risk  
2 factors and Alzheimer's disease: are these risk factors for plaques and tangles or for  
3 concomitant vascular pathology that increases the likelihood of dementia? An  
4 evidence-based review. *Alzheimers Res Ther.*4(1):1.
- 5 11. Craggs LJ, Fenwick R, Oakley AE, Ihara M, Kalara RN (2015)  
6 Immunolocalization of platelet-derived growth factor receptor-beta (PDGFR-beta) and  
7 pericytes in cerebral autosomal dominant arteriopathy with subcortical infarcts and  
8 leukoencephalopathy (CADASIL). *Neuropathol Appl Neurobiol.*41(4):557-70.
- 9 12. Dizon ML, Maa T, Kessler JA (2011) The bone morphogenetic protein  
10 antagonist noggin protects white matter after perinatal hypoxia-ischemia. *Neurobiol*  
11 *Dis.*42(3):318-26.
- 12 13. Erkinjuntti T, Benavente O, Eliasziw M, Munoz DG, Sulkava R, Haltia M,  
13 Hachinski V (1996) Diffuse vacuolization (spongiosis) and arteriolosclerosis in the  
14 frontal white matter occurs in vascular dementia. *Arch Neurol.*53(4):325-32.
- 15 14. Fuller ML, DeChant AK, Rothstein B, Caprariello A, Wang R, Hall AK, Miller  
16 RH (2007) Bone morphogenetic proteins promote gliosis in demyelinating spinal cord  
17 lesions. *Ann Neurol.*62(3):288-300.
- 18 15. Gomes WA, Mehler MF, Kessler JA (2003) Transgenic overexpression of  
19 BMP4 increases astroglial and decreases oligodendroglial lineage commitment. *Dev*  
20 *Biol.*255(1):164-77.
- 21 16. Grinspan JB, Edell E, Carpio DF, Beesley JS, Lavy L, Pleasure D, Golden JA  
22 (2000) Stage-specific effects of bone morphogenetic proteins on the oligodendrocyte  
23 lineage. *J Neurobiol.*43(1):1-17.
- 24 17. Gross RE, Mehler MF, Mabie PC, Zang Z, Santschi L, Kessler JA (1996) Bone

- 1 morphogenetic proteins promote astroglial lineage commitment by mammalian  
2 subventricular zone progenitor cells. *Neuron*.17(4):595-606.
- 3 18. Hara K, Shiga A, Fukutake T, Nozaki H, Miyashita A, Yokoseki A, Kawata H,  
4 Koyama A, Arima K, Takahashi T, Ikeda M, Shiota H, Tamura M, Shimoe Y, Hirayama  
5 M, Arisato T, Yanagawa S, Tanaka A, Nakano I, Ikeda S, Yoshida Y, Yamamoto T,  
6 Ikeuchi T, Kuwano R, Nishizawa M, Tsuji S, Onodera O (2009) Association of HTRA1  
7 mutations and familial ischemic cerebral small-vessel disease. *N Engl J*  
8 *Med*.360(17):1729-39.
- 9 19. Iadecola C (2013) The pathobiology of vascular dementia.  
10 *Neuron*.80(4):844-66.
- 11 20. Ihara M, Polvikoski TM, Hall R, Slade JY, Perry RH, Oakley AE, Englund E,  
12 O'Brien JT, Ince PG, Kalaria RN (2010) Quantification of myelin loss in frontal lobe  
13 white matter in vascular dementia, Alzheimer's disease, and dementia with Lewy bodies.  
14 *Acta Neuropathol*.119(5):579-89.
- 15 21. Ihara M, Yamamoto Y (2016) Emerging Evidence for Pathogenesis of Sporadic  
16 Cerebral Small Vessel Disease. *Stroke*.47(2):554-60.
- 17 22. Jellinger KA (2007) The enigma of vascular cognitive disorder and vascular  
18 dementia. *Acta Neuropathol*.113(4):349-88.
- 19 23. Jellinger KA (2013) Pathology and pathogenesis of vascular cognitive  
20 impairment-a critical update. *Front Aging Neurosci*.5:17.
- 21 24. Kalaria RN, Kenny RA, Ballard CG, Perry R, Ince P, Polvikoski T (2004)  
22 Towards defining the neuropathological substrates of vascular dementia. *J Neurol*  
23 *Sci*.226(1-2):75-80.
- 24 25. Kamouchi M, Ago T, Kuroda J, Kitazono T (2012) The possible roles of brain

- 1 pericytes in brain ischemia and stroke. *Cell Mol Neurobiol.*32(2):159-65.
- 2 26. Kan L, Kitterman JA, Procissi D, Chakkalakal S, Peng CY, McGuire TL,  
3 Goldsby RE, Pignolo RJ, Shore EM, Kaplan FS, Kessler JA (2012) CNS demyelination  
4 in fibrodysplasia ossificans progressiva. *J Neurol.*259(12):2644-55.
- 5 27. Mabie PC, Mehler MF, Marmur R, Papavasiliou A, Song Q, Kessler JA (1997)  
6 Bone morphogenetic proteins induce astroglial differentiation of  
7 oligodendroglial-astroglial progenitor cells. *J Neurosci.*17(11):4112-20.
- 8 28. Maesako M, Uemura M, Tashiro Y, Sasaki K, Watanabe K, Noda Y, Ueda K,  
9 Asada-Utsugi M, Kubota M, Okawa K, Ihara M, Shimohama S, Uemura K, Kinoshita A  
10 (2015) High Fat Diet Enhances beta-Site Cleavage of Amyloid Precursor Protein (APP)  
11 via Promoting beta-Site APP Cleaving Enzyme 1/Adaptor Protein 2/Clathrin Complex  
12 Formation. *PLoS One.*10(9):e0131199.
- 13 29. Maki T, Ihara M, Fujita Y, Nambu T, Miyashita K, Yamada M, Washida K,  
14 Nishio K, Ito H, Harada H, Yokoi H, Arai H, Itoh H, Nakao K, Takahashi R, Tomimoto  
15 H (2011) Angiogenic and vasoprotective effects of adrenomedullin on prevention of  
16 cognitive decline after chronic cerebral hypoperfusion in mice. *Stroke.*42(4):1122-8.
- 17 30. Maki T, Maeda M, Uemura M, Lo EK, Terasaki Y, Liang AC, Shindo A, Choi  
18 YK, Taguchi A, Matsuyama T, Takahashi R, Ihara M, Arai K (2015) Potential  
19 interactions between pericytes and oligodendrocyte precursor cells in perivascular  
20 regions of cerebral white matter. *Neurosci Lett.*597:164-9.
- 21 31. Mazaheri Z, Movahedin M, Rahbarizadeh F, Amanpour S (2011) Different  
22 doses of bone morphogenetic protein 4 promote the expression of early germ  
23 cell-specific gene in bone marrow mesenchymal stem cells. *In Vitro Cell Dev Biol*  
24 *Anim.*47(8):521-5.

- 1 32. Mirra SS, Heyman A, McKeel D, Sumi SM, Crain BJ, Brownlee LM, Vogel FS,  
2 Hughes JP, van Belle G, Berg L (1991) The Consortium to Establish a Registry for  
3 Alzheimer's Disease (CERAD). Part II. Standardization of the neuropathologic  
4 assessment of Alzheimer's disease. *Neurology*.41(4):479-86.
- 5 33. Miyamoto N, Tanaka R, Shimura H, Watanabe T, Mori H, Onodera M,  
6 Mochizuki H, Hattori N, Urabe T (2010) Phosphodiesterase III inhibition promotes  
7 differentiation and survival of oligodendrocyte progenitors and enhances regeneration  
8 of ischemic white matter lesions in the adult mammalian brain. *J Cereb Blood Flow*  
9 *Metab*.30(2):299-310.
- 10 34. Nicolakakis N, Hamel E (2011) Neurovascular function in Alzheimer's disease  
11 patients and experimental models. *J Cereb Blood Flow Metab*.31(6):1354-70.
- 12 35. Okamoto Y, Yamamoto T, Kalaria RN, Senzaki H, Maki T, Hase Y, Kitamura A,  
13 Washida K, Yamada M, Ito H, Tomimoto H, Takahashi R, Ihara M (2012) Cerebral  
14 hypoperfusion accelerates cerebral amyloid angiopathy and promotes cortical  
15 microinfarcts. *Acta Neuropathol*.123(3):381-94.
- 16 36. Reid MV, Murray KA, Marsh ED, Golden JA, Simmons RA, Grinspan JB  
17 (2012) Delayed myelination in an intrauterine growth retardation model is mediated by  
18 oxidative stress upregulating bone morphogenetic protein 4. *J Neuropathol Exp*  
19 *Neurol*.71(7):640-53.
- 20 37. Renner O, Tsimpas A, Kostin S, Valable S, Petit E, Schaper W, Marti HH  
21 (2003) Time- and cell type-specific induction of platelet-derived growth factor  
22 receptor-beta during cerebral ischemia. *Brain Res Mol Brain Res*.113(1-2):44-51.
- 23 38. Ronnema E, Zethelius B, Lannfelt L, Kilander L (2011) Vascular risk factors  
24 and dementia: 40-year follow-up of a population-based cohort. *Dement Geriatr Cogn*



- 1 Disord.31(6):460-6.
- 2 39. Rosenberg GA, Wallin A, Wardlaw JM, Markus HS, Montaner J, Wolfson L,  
3 Iadecola C, Zlokovic BV, Joutel A, Dichgans M, Duering M, Schmidt R, Korczyn AD,  
4 Grinberg LT, Chui HC, Hachinski V (2016) Consensus statement for diagnosis of  
5 subcortical small vessel disease. *J Cereb Blood Flow Metab.*36(1):6-25.
- 6 40. Ruitenbergh A, den Heijer T, Bakker SL, van Swieten JC, Koudstaal PJ, Hofman  
7 A, Breteler MM (2005) Cerebral hypoperfusion and clinical onset of dementia: the  
8 Rotterdam Study. *Ann Neurol.*57(6):789-94.
- 9 41. Russell R, Perkhofer L, Liebau S, Lin Q, Lechel A, Feld FM, Hessmann E,  
10 Gaedcke J, Guthle M, Zenke M, Hartmann D, von Figura G, Weissinger SE, Rudolph  
11 KL, Moller P, Lennerz JK, Seufferlein T, Wagner M, Kleger A (2015) Loss of ATM  
12 accelerates pancreatic cancer formation and epithelial-mesenchymal transition. *Nat*  
13 *Commun.*6:7677.
- 14 42. Sabo JK, Aumann TD, Kilpatrick TJ, Cate HS (2013) Investigation of  
15 sequential growth factor delivery during cuprizone challenge in mice aimed to enhance  
16 oligodendroglial myelination and myelin repair. *PLoS One.*8(5):e63415.
- 17 43. Sabo JK, Aumann TD, Merlo D, Kilpatrick TJ, Cate HS (2011) Remyelination  
18 is altered by bone morphogenetic protein signaling in demyelinated lesions. *J*  
19 *Neurosci.*31(12):4504-10.
- 20 44. Samanta J, Alden T, Gobeske K, Kan L, Kessler JA (2010) Noggin protects  
21 against ischemic brain injury in rodents. *Stroke.*41(2):357-62.
- 22 45. See JM, Grinspan JB (2009) Sending mixed signals: bone morphogenetic  
23 protein in myelination and demyelination. *J Neuropathol Exp Neurol.*68(6):595-604.
- 24 46. Sengillo JD, Winkler EA, Walker CT, Sullivan JS, Johnson M, Zlokovic BV

- 1 (2013) Deficiency in mural vascular cells coincides with blood-brain barrier disruption  
2 in Alzheimer's disease. *Brain Pathol.*23(3):303-10.
- 3 47. Seo JH, Maki T, Maeda M, Miyamoto N, Liang AC, Hayakawa K, Pham LD,  
4 Suwa F, Taguchi A, Matsuyama T, Ihara M, Kim KW, Lo EH, Arai K (2014)  
5 Oligodendrocyte precursor cells support blood-brain barrier integrity via TGF-beta  
6 signaling. *PLoS One.*9(7):e103174.
- 7 48. Shibata M, Ohtani R, Ihara M, Tomimoto H (2004) White matter lesions and  
8 glial activation in a novel mouse model of chronic cerebral hypoperfusion.  
9 *Stroke.*35(11):2598-603.
- 10 49. Sofroniew MV, Vinters HV (2010) Astrocytes: biology and pathology. *Acta*  
11 *Neuropathol.*119(1):7-35.
- 12 50. Song S, Ewald AJ, Stallcup W, Werb Z, Bergers G (2005) PDGFRbeta+  
13 perivascular progenitor cells in tumours regulate pericyte differentiation and vascular  
14 survival. *Nat Cell Biol.*7(9):870-9.
- 15 51. Sweeney MD, Ayyadurai S, Zlokovic BV (2016) Pericytes of the neurovascular  
16 unit: key functions and signaling pathways. *Nat Neurosci.*19(6):771-83.
- 17 52. Thirumangalakudi L, Samany PG, Owoso A, Wiskar B, Grammas P (2006)  
18 Angiogenic proteins are expressed by brain blood vessels in Alzheimer's disease. *J*  
19 *Alzheimers Dis.*10(1):111-8.
- 20 53. Vicente Lopez MA, Vazquez Garcia MN, Entrena A, Olmedillas Lopez S,  
21 Garcia-Arranz M, Garcia-Olmo D, Zapata A (2011) Low doses of bone morphogenetic  
22 protein 4 increase the survival of human adipose-derived stem cells maintaining their  
23 stemness and multipotency. *Stem Cells Dev.*20(6):1011-9.
- 24 54. Wardlaw JM, Smith C, Dichgans M (2013) Mechanisms of sporadic cerebral

- 1 small vessel disease: insights from neuroimaging. *Lancet Neurol.*12(5):483-97.
- 2 55. Winkler EA, Bell RD, Zlokovic BV (2011) Central nervous system pericytes in  
3 health and disease. *Nat Neurosci.*14(11):1398-405.
- 4 56. Winkler EA, Sengillo JD, Sullivan JS, Henkel JS, Appel SH, Zlokovic BV  
5 (2013) Blood-spinal cord barrier breakdown and pericyte reductions in amyotrophic  
6 lateral sclerosis. *Acta Neuropathol.*125(1):111-20.
- 7 57. Wu M, Hernandez M, Shen S, Sabo JK, Kelkar D, Wang J, O'Leary R, Phillips  
8 GR, Cate HS, Casaccia P (2012) Differential modulation of the oligodendrocyte  
9 transcriptome by sonic hedgehog and bone morphogenetic protein 4 via opposing  
10 effects on histone acetylation. *J Neurosci.*32(19):6651-64.
- 11 58. Yamamoto Y, Ihara M, Tham C, Low RW, Slade JY, Moss T, Oakley AE,  
12 Polvikoski T, Kalaria RN (2009) Neuropathological correlates of temporal pole white  
13 matter hyperintensities in CADASIL. *Stroke.*40(6):2004-11.
- 14 59. Zlokovic BV (2011) Neurovascular pathways to neurodegeneration in  
15 Alzheimer's disease and other disorders. *Nat Rev Neurosci.*12(12):723-38.

**Table 1.** Demographics of subjects and pathological analysis

	No.	Age	Sex	BW(g)	SP	NFT	FMI	Clinical and pathological diagnosis
Control	1	68	M	1400	None	0	79.7	ALS
	2	71	F	1280	Sparse	I	78.0	ALS
	3	75	M	1090	Sparse	I	97.1	Emphysema
	4	70	F	1030	None	0	72.4	Schizophrenia
	5	80	F	1150	Sparse	I	67.8	ALS
	6	79	M	-	Sparse	I	90.2	ALS
AD	7	80	F	-	Frequent	V	54.0	AD
	8	85	M	1060	Frequent	IV	79.5	AD
	9	67	F	940	Frequent	VI	74.4	AD
	10	84	F	1080	Frequent	VI	67.6	AD
	11	93	F	1150	Frequent	VI	74.8	AD
	12	77	M	1050	Frequent	VI	78.5	AD
SVD	13	80	M	1120	None	0	46.5	SVD
	14	70	M	1200	Sparse	II	61.6	SVD
	15	86	F	940	Sparse	III	55.9	SVD
	16	76	F	1100	None	III	59.9	SVD
	17	90	M	-	Sparse	III	47.8	SVD
	18	82	M	1050	Sparse	I	53.5	SVD
	19	82	F	1200	Sparse	III	68.5	SVD

1  
2  
3  
4  
5  
6  
7  
8  
9  
10  
11  
12  
13  
14  
15  
16  
17  
18  
19  
20  
21  
22  
23  
24  
25  
26  
27  
28  
29  
30  
31  
32  
33  
34  
35  
36  
37  
38  
39  
40  
41  
42  
43  
44  
45  
46  
47  
48  
49  
50  
51  
52  
53  
54  
55  
56  
57  
58  
59  
60

AD, Alzheimer’s disease; ALS, amyotrophic lateral sclerosis; BW, brain weight; FMI, frontal myelin index; NFT, neurofibrillary tangle; SP, senile plaque; SVD, small vessel disease

For Peer Review Only

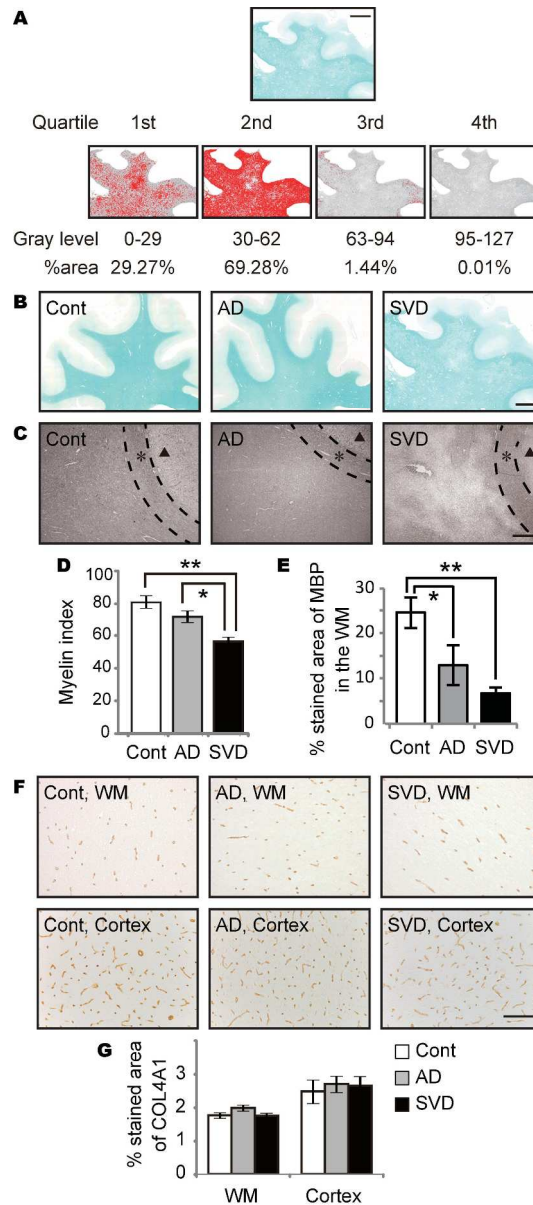


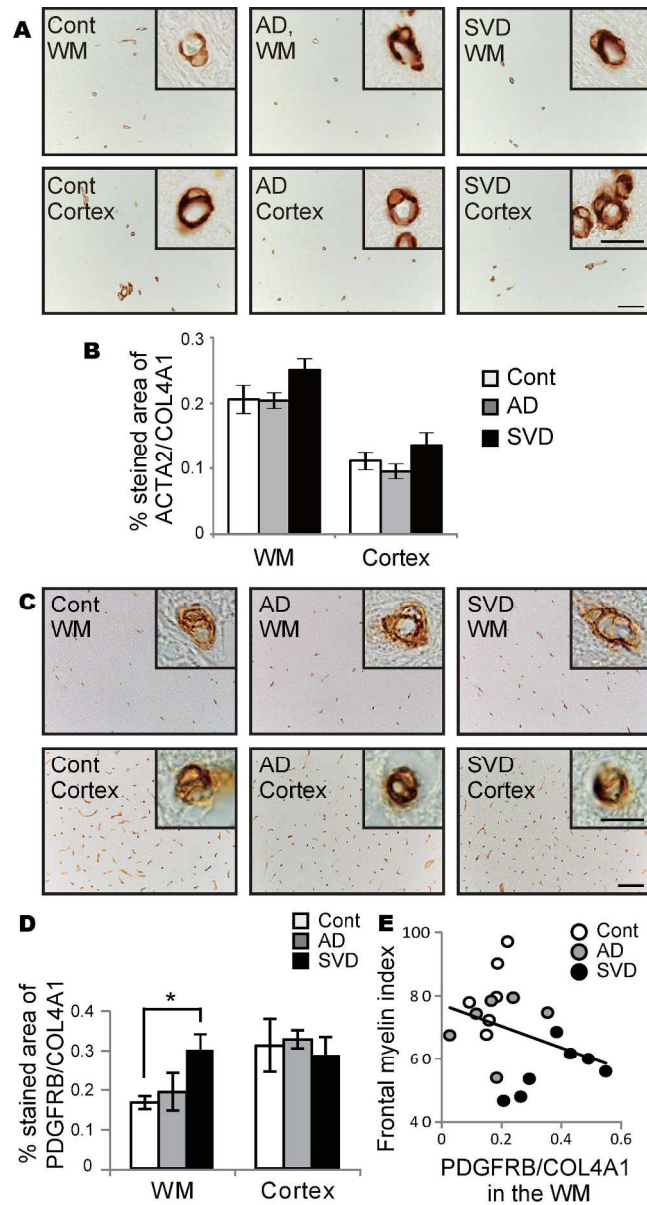
**Figure 1. Degree of myelin loss and capillary bed density in the frontal lobes of post-mortem human brain samples.** (A) A procedure for calculating myelin index. The median gray level of each quartile (14.5, 46.0, 78.5, and 111.0) is multiplied by percent area in each quartile (29.27%, 69.28%, 1.44%, and 0.01%), and summed up to be 37.25 as the myelin index for the representative image of LFB staining. *Bar* indicates 5 mm. (B) Representative images of LFB staining in control, AD, and SVD cases. *Bar* indicates 5 mm. (C) Representative images of MBP staining (myelin) in control, AD, and SVD cases. *Bar* indicates 400  $\mu$ m. *Black triangles* indicate cortex. *Asterisks* mean U-fiber. (D) Myelin index calculated from each LFB staining of all three groups. Differences are significant between any two groups, except between control and AD: control vs. AD,  $P = 0.226$ ; control vs. SVD,  $**P = 0.001$ ; AD vs. SVD,  $*P = 0.027$ . (E) The percentage of MBP in the WM in all three groups. Differences are significant between any two groups, except between AD and SVD: control vs. AD,  $*P = 0.027$ ; control vs. SVD,  $**P = 0.001$ ; AD vs. SVD,  $P = 0.224$ . (F) Representative images of COL4A1 staining (basement membrane marker) in control, AD, and SVD cases. *Bar* indicates 100  $\mu$ m. (G) The percentage of COL4A1 in the WM and cortex in all three groups. Differences

1  
2  
3  
4  
5  
6  
7  
8  
9  
10  
11  
12  
13  
14  
15  
16  
17  
18  
19  
20  
21  
22  
23  
24  
25  
26  
27  
28  
29  
30  
31  
32  
33  
34  
35  
36  
37  
38  
39  
40  
41  
42  
43  
44  
45  
46  
47  
48  
49  
50  
51  
52  
53  
54  
55  
56  
57  
58  
59  
60

are not significant in the WM ( $P = 0.095$ ) and cortex ( $P = 0.095$ ). *Vertical bars* represent mean  $\pm$  SEM. Abbreviations are as follows: AD, Alzheimer's disease; Cont, control; MBP, myelin basic protein; LFB, Luxol fast blue; SVD, small vessel disease; WM, white matter.

Figure 1  
200x452mm (300 x 300 DPI)

For Peer Review Only



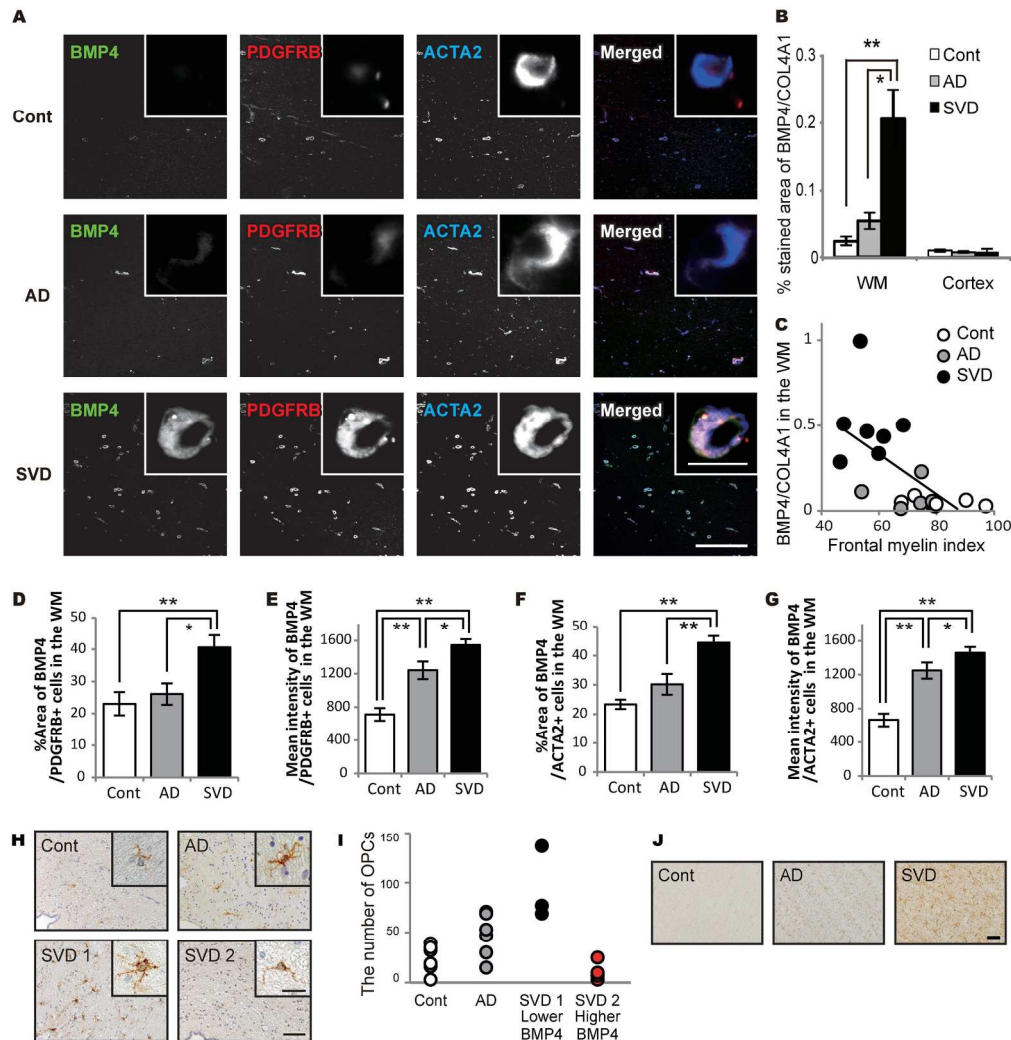
**Figure 2. Pericyte density as assessed by ACTA2 and PDGFRB labeling in the post-mortem human brain samples.** (A) Representative images of ACTA2 staining in control, AD, and SVD cases. *Insets* show ACTA2-positive pericytes. *Bars* indicate 100  $\mu$ m and 10  $\mu$ m (*insets*). (B) The percentage of ACTA2 in the WM and cortex in all three groups. Differences are not significant in the WM ( $P = 0.123$ ) and cortex ( $P = 0.220$ ). (C) Representative images of PDGFRB staining in control, AD, and SVD cases. *Insets* show PDGFRB-positive pericytes. *Bars* indicate 100  $\mu$ m and 10  $\mu$ m (*insets*). (D) The percentage of PDGFRB in the WM and cortex in all three groups. Differences are significant between control and SVD in the WM: control vs. AD,  $P = 0.955$ ; control vs. SVD,  $*P = 0.046$ ; AD vs. SVD,  $P = 0.081$ . Differences are not significant in the cortex ( $P = 0.464$ ). (E) An inverse correlation between the percentage of PDGFRB and the myelin index all 19 cases combined ( $r = -0.568$ ,  $*P = 0.013$ ). *Vertical bars* represent mean  $\pm$  SEM. Abbreviations are as follows: AD, Alzheimer's disease; Cont, control; SVD, small vessel disease; WM, white matter.

Figure 2  
165x309mm (300 x 300 DPI)



1  
2  
3  
4  
5  
6  
7  
8  
9  
10  
11  
12  
13  
14  
15  
16  
17  
18  
19  
20  
21  
22  
23  
24  
25  
26  
27  
28  
29  
30  
31  
32  
33  
34  
35  
36  
37  
38  
39  
40  
41  
42  
43  
44  
45  
46  
47  
48  
49  
50  
51  
52  
53  
54  
55  
56  
57  
58  
59  
60

For Peer Review Only



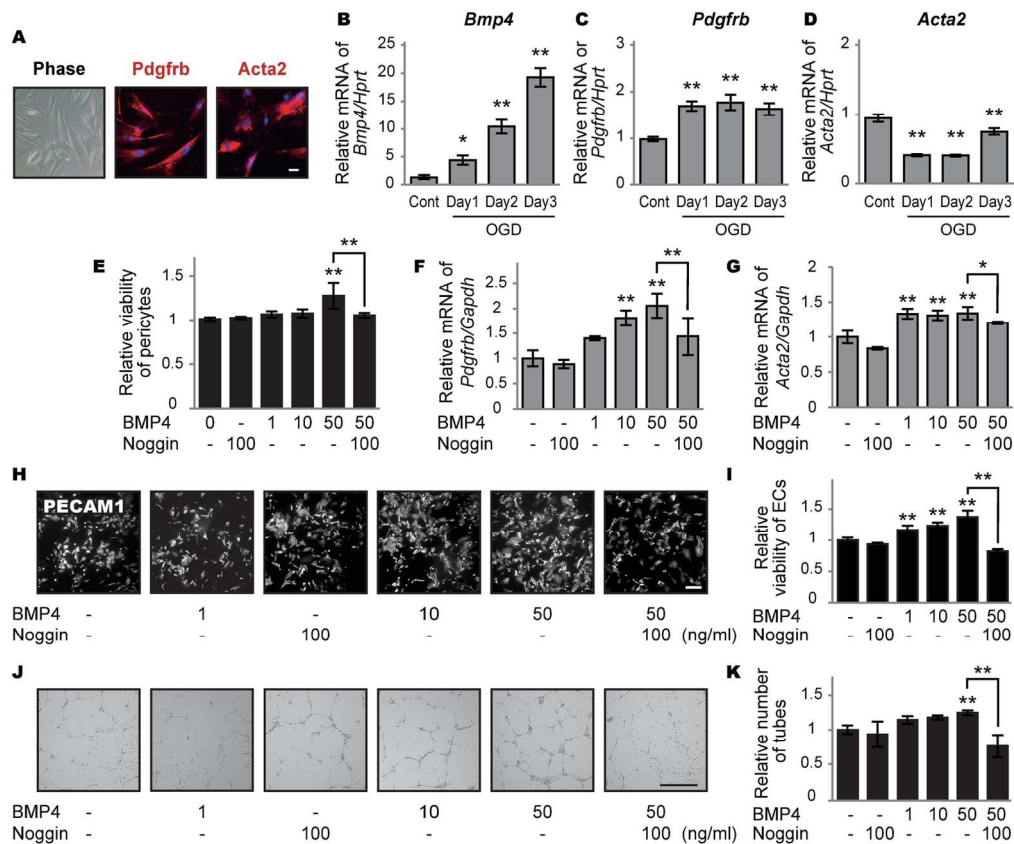
**Figure 3. Pericyte BMP4 expression in damaged white matter in the post-mortem human brain samples.** (A) Representative triple-immunofluorescent images for BMP4, PDGFRB, and ACTA2, and their merged images in the WM of all three groups. *Insets* show enlarged pericytes. *Bars* indicate 100  $\mu$ m and 10  $\mu$ m (*insets*). (B) The percentage of BMP4 expression in all three groups. Differences are significant between any two groups, except between control and AD in the WM: control vs. AD,  $P = 0.804$ ; control vs. SVD,  $**P = 0.003$ ; AD vs. SVD,  $*P = 0.012$ . Differences are not significant in the cortex ( $P = 0.659$ ). (C) An inverse correlation between the percentage of BMP4 expression and the myelin index in all 19 cases combined ( $r = -0.549$ ,  $*P = 0.015$ ). (D) The percent area of BMP4 expression in PDGFRB-positive cells in the WM of all three groups. Differences are significant between any two groups, except between control and AD: control vs. AD,  $P = 0.593$ ; control vs. SVD,  $**P = 0.001$ ; AD vs. SVD,  $*P = 0.011$ . (E) The mean intensity of BMP4 in PDGFRB-positive cells in the WM of all three groups. Differences are significant between any two groups: control vs. AD,  $**P < 0.001$ ; control vs. SVD,  $**P < 0.001$ ; AD vs. SVD,  $*P = 0.017$ . (F) The percent area of BMP4 expression in ACTA2-positive cells in the WM of all three groups. Differences are significant between any two groups, except between control and AD: control vs. AD,  $P = 0.079$ ; control vs. SVD,  $**P < 0.001$ ; AD vs. SVD,  $**P < 0.001$ . (G) The mean intensity of BMP4 in ACTA2-positive cells in the WM of all three groups. Differences are significant between any two groups: control vs. AD,  $**P < 0.001$ ; control vs. SVD,  $**P < 0.001$ ; AD vs. SVD,  $*P = 0.018$ . (H) Representative images of PDGFRA expression in the interstitium of the SVZ in the cases of control, AD, and SVD of post-mortem human brain samples. According to expression levels of BMP4 (BMP4-to-COL4A1 ratio), the SVD cases are further classified into subgroup: a

1  
2  
3 lower BMP-4 expressing group (SVD 1) and a higher one (SVD 2) with the cut-off ratio of 0.31. *Insets* show  
4 enlarged images of OPCs. *Bars* indicate 50  $\mu\text{m}$  and 10  $\mu\text{m}$  (insets). (I) The number of OPCs in all 4 groups.  
5 SVD 2 group shows smaller number of OPCs compared with SVD 1 group. (J) Representative images of  
6 GFAP expression in the WM of post-mortem human brain samples. The WM of SVD shows severe astrogliosis  
7 with high GFAP expression. *Bar* indicates 50  $\mu\text{m}$ . *Vertical bars* represent mean  $\pm$  SEM. Abbreviations are as  
8 follows: AD, Alzheimer's disease; Cont, control; SVD, small vessel disease; WM, white matter.

9 Figure 3  
10 187x194mm (300 x 300 DPI)

11  
12  
13  
14  
15  
16  
17  
18  
19  
20  
21  
22  
23  
24  
25  
26  
27  
28  
29  
30  
31  
32  
33  
34  
35  
36  
37  
38  
39  
40  
41  
42  
43  
44  
45  
46  
47  
48  
49  
50  
51  
52  
53  
54  
55  
56  
57  
58  
59  
60

For Peer Review Only



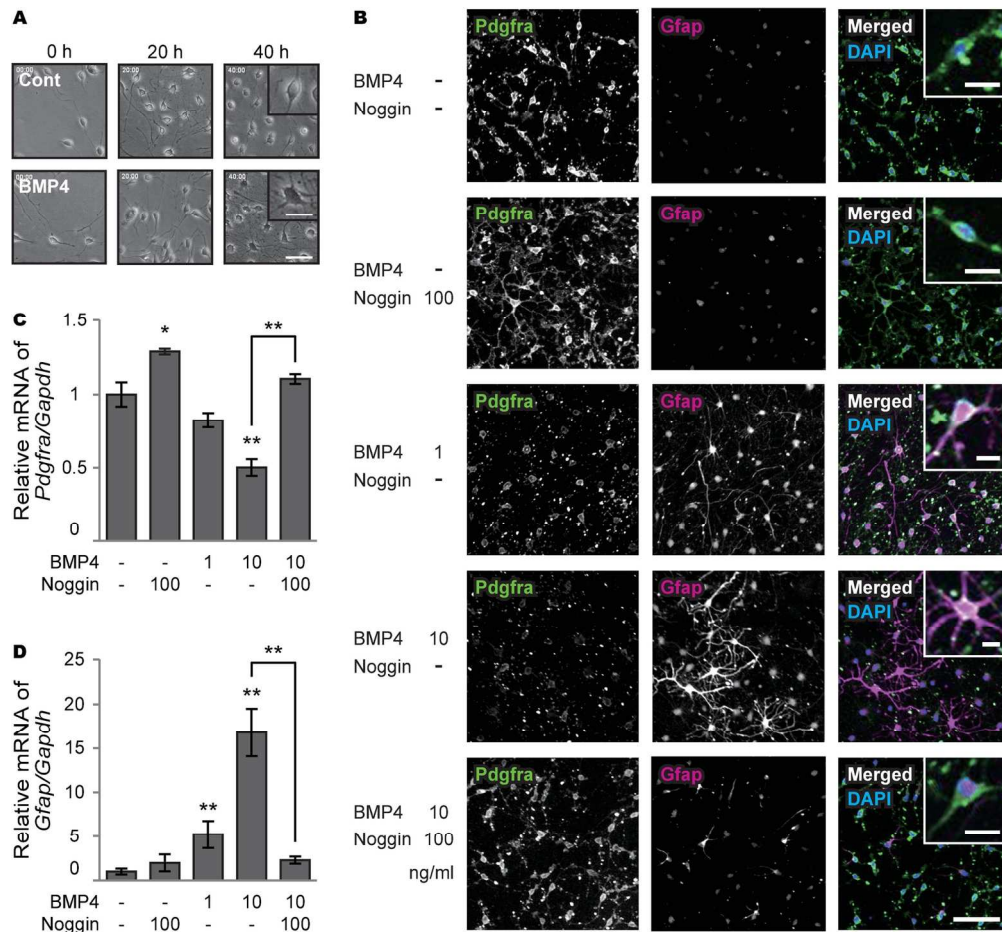
**Figure 3. Pericyte BMP4 expression in damaged white matter in the post-mortem human brain samples.** (A) Representative triple-immunofluorescent images for BMP4, PDGFRB, and ACTA2, and their merged images in the WM of all three groups. *Insets* show enlarged pericytes. *Bars* indicate 100  $\mu$ m and 10  $\mu$ m (*insets*). (B) The percentage of BMP4 expression in all three groups. Differences are significant between any two groups, except between control and AD in the WM: control vs. AD,  $P = 0.804$ ; control vs. SVD,  $**P = 0.003$ ; AD vs. SVD,  $*P = 0.012$ . Differences are not significant in the cortex ( $P = 0.659$ ). (C) An inverse correlation between the percentage of BMP4 expression and the myelin index in all 19 cases combined ( $r = -0.549$ ,  $*P = 0.015$ ). (D) The percent area of BMP4 expression in PDGFRB-positive cells in the WM of all three groups. Differences are significant between any two groups, except between control and AD: control vs. AD,  $P = 0.593$ ; control vs. SVD,  $**P = 0.001$ ; AD vs. SVD,  $*P = 0.011$ . (E) The mean intensity of BMP4 in PDGFRB-positive cells in the WM of all three groups. Differences are significant between any two groups: control vs. AD,  $**P < 0.001$ ; control vs. SVD,  $**P < 0.001$ ; AD vs. SVD,  $*P = 0.017$ . (F) The percent area of BMP4 expression in ACTA2-positive cells in the WM of all three groups. Differences are significant between any two groups, except between control and AD: control vs. AD,  $P = 0.079$ ; control vs. SVD,  $**P < 0.001$ ; AD vs. SVD,  $**P < 0.001$ . (G) The mean intensity of BMP4 in ACTA2-positive cells in the WM of all three groups. Differences are significant between any two groups: control vs. AD,  $**P < 0.001$ ; control vs. SVD,  $**P < 0.001$ ; AD vs. SVD,  $*P = 0.018$ . (H) Representative images of PDGFRA expression in the interstitium of the SVZ in the cases of control, AD, and SVD of post-mortem human brain samples. According to expression levels of BMP4 (BMP4-to-COL4A1 ratio), the SVD cases are further classified into subgroup: a lower BMP-4 expressing group (SVD 1) and a higher one (SVD 2) with the cut-off ratio of 0.31. *Insets* show enlarged images of OPCs. *Bars* indicate 50  $\mu$ m and 10  $\mu$ m (*insets*). (I) The number of OPCs in all 4 groups. SVD 2 group shows smaller number of OPCs compared with SVD 1 group. (J) Representative images of GFAP expression in the WM of post-mortem human brain samples. The WM of SVD shows severe astrogliosis with high GFAP expression. *Bar* indicates 50  $\mu$ m. *Vertical bars* represent mean  $\pm$  SEM. Abbreviations are as follows: AD, Alzheimer's disease; Cont, control; SVD, small vessel disease; WM, white matter.

Figure 4

1  
2  
3  
4  
5  
6  
7  
8  
9  
10  
11  
12  
13  
14  
15  
16  
17  
18  
19  
20  
21  
22  
23  
24  
25  
26  
27  
28  
29  
30  
31  
32  
33  
34  
35  
36  
37  
38  
39  
40  
41  
42  
43  
44  
45  
46  
47  
48  
49  
50  
51  
52  
53  
54  
55  
56  
57  
58  
59  
60

148x123mm (300 x 300 DPI)

For Peer Review Only



**Figure 5. Effects of BMP4 on cultured oligodendrocyte precursor cells.** (A) Time-lapse images of primary OPCs in proliferation media with or without BMP4. *Insets* show enlarged images. *Bars* indicate 100  $\mu\text{m}$  and 50  $\mu\text{m}$  (*insets*). (B) Representative triple-immunofluorescent images for *Pdgfra* and *Gfap*, and their merged images with DAPI for nuclear staining. *Insets* show enlarged images. *Bars* indicate 50  $\mu\text{m}$  and 10  $\mu\text{m}$  (*insets*). (C, D) Relative mRNA levels of *Pdgfra* and *Gfap* in the proliferation assay. (C) BMP4 decreases *Pdgfra* mRNA levels in a dose-dependent manner ( $P = 0.062$  for 1 ng/ml and  $**P < 0.001$  for 10 ng/ml), which is blocked by noggin ( $**P = 0.001$ ). Treatment with noggin alone increases *Pdgfra* mRNA levels ( $*P = 0.015$ ). (D) BMP4 significantly increases *Gfap* mRNA expression in a dose-dependent manner ( $**P = 0.004$  for 1 ng/ml and  $**P < 0.001$  for 1 and 10 ng/ml), which is blocked by noggin ( $**P < 0.001$ ). *Vertical bars* represent mean  $\pm$  SD. Abbreviations are as follows: Cont, control; *Gapdh*, glyceraldehyde-3-phosphate dehydrogenase.

Figure 5

159x148mm (300 x 300 DPI)



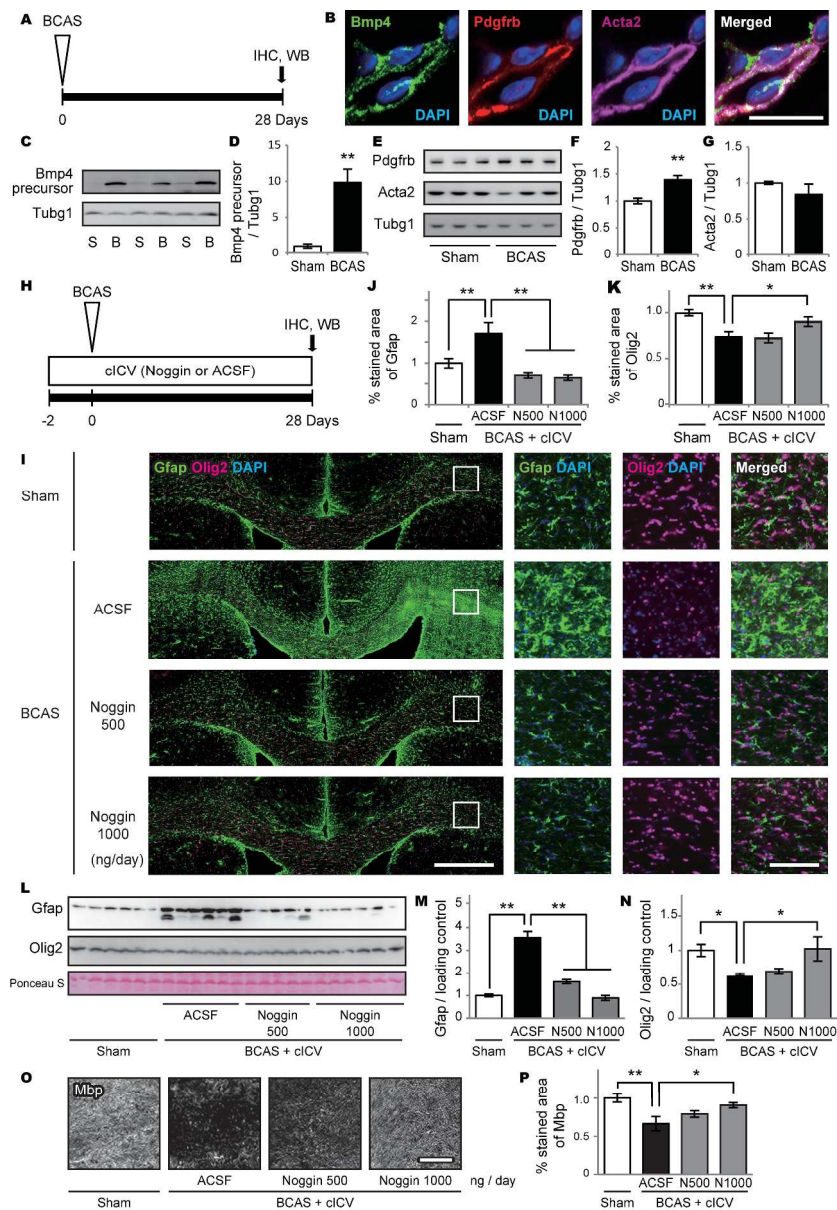


**Figure 6. BMP4 expression and effect of noggin in the mouse brain after chronic hypoperfusion.**

(A) Experimental design of the first trial. Adult mice subjected to BCAS are analyzed by immunohistochemistry and western blot. (B) Representative triple-immunofluorescent images for Bmp4, Pdgfrb, and Acta2, and their merged images with DAPI for nuclear staining. Bars indicate 10  $\mu$ m. (C-G) Western blot shows significantly increased Bmp4 precursor (C, D) and Pdgfrb (E, F) levels after BCAS (\*\* $P = 0.002$  for Bmp4 precursor and \*\* $P = 0.004$  for Pdgfrb), with not significantly changes in Acta2 levels ( $P = 0.660$ ) (E, G). (H) Experimental design of the second trial. Adult mice subjected to BCAS receive noggin (500 ng/day or 1000 ng/day) in ACSF or ACSF only through cICV two days prior to BCAS, are euthanized and their brains analyzed by immunohistochemistry and western blot. (I) Representative immunofluorescent images of Gfap and Olig2 with DAPI (the leftmost images) and their enlarged images (three right images). Bars indicate 500  $\mu$ m (left) and 100  $\mu$ m (right). (J) Semiquantitative analysis of immunofluorescent images shows that BCAS significantly increases GFAP-positive cells (\*\* $P = 0.004$ ), which is strongly suppressed by noggin cICV (\*\* $P < 0.001$  for both 500 ng/day and 1000 ng/day). (K) Semiquantitative analysis of

1  
2  
3 immunofluorescent images shows BCAS significantly decreases Olig2-positive cells (\*\* $P < 0.001$ ), which is  
4 significantly ameliorated by high dose of noggin cICV ( $P = 0.771$  for 500 ng/day and \* $P = 0.026$  for 1000  
5 ng/day). (L, M) Western blot shows significantly increased Gfap levels after BCAS (\*\* $P < 0.001$  for Sham vs.  
6 BCAS + ACSF), which is suppressed by noggin cICV (\*\* $P < 0.001$  for BCAS + ACSF vs. BCAS + noggin 500  
7 and 1000 ng/day) (L, N). Western blot shows significantly decreased Olig2 levels after BCAS (\* $P = 0.030$  for  
8 Sham vs. BCAS + ACSF), which is ameliorated by a high dose of noggin cICV ( $P = 0.698$  for BCAS + ACSF  
9 vs. BCAS + noggin 500 ng/day; and \* $P = 0.042$  for BCAS + ACSF vs. BCAS + noggin 1000 ng/day). (O, P)  
10 Semiquantitative analysis of immunofluorescent images shows that BCAS significantly decreases Mbp (\*\* $P =$   
11  $0.001$ ), which is significantly ameliorated by high dose of noggin cICV ( $P = 0.169$  for 500 ng/day and \* $P =$   
12  $0.034$  for 1000 ng/day). *Vertical bars* represent mean  $\pm$  SEM. Abbreviations are as follows: B, BCAS; cICV,  
13 continuous intracerebroventricular infusion; IHC, immunohistochemistry; N500, noggin 500 ng/day; N1000,  
14 noggin 1000 ng/day; S, Sham operation; Tubb1, tubulin gamma 1, also known as gamma tubulin; WB,  
15 western blot.

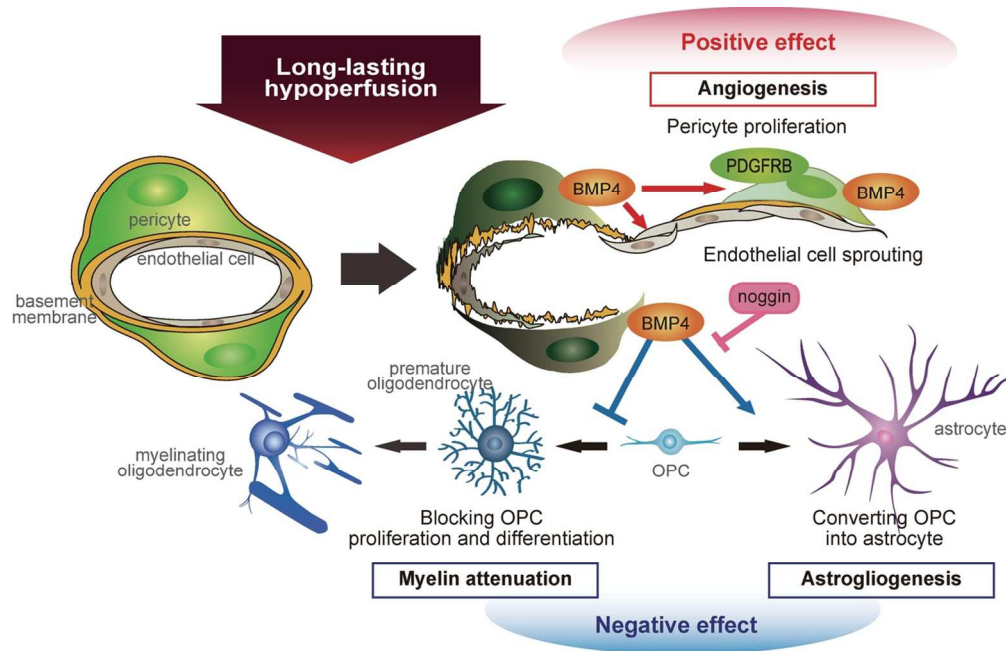
Figure 6

263x382mm (300 x 300 DPI)

16  
17  
18  
19  
20  
21  
22  
23  
24  
25  
26  
27  
28  
29  
30  
31  
32  
33  
34  
35  
36  
37  
38  
39  
40  
41  
42  
43  
44  
45  
46  
47  
48  
49  
50  
51  
52  
53  
54  
55  
56  
57  
58  
59  
60

or Peer Review Only





29  
30  
31  
32  
33  
34

**Figure 7. Putative scheme for BMP4 effect on multiple cell lineages after chronic ischemia.** BMP4 generated from pericytes after hypoperfusion may promote compensatory angiogenesis by significantly increasing production of endothelial cells and pericytes. However, BMP4 expression may also induce astrogliogenesis at the expense of OPC proliferation and maturation, thereby aggravating white matter damage. Noggin has the potential to suppress BMP4-induced astrogliogenesis and rescue oligodendrogenesis.

Figure 7  
115x74mm (300 x 300 DPI)

## Supplementary Materials

### Uemura, et al.: **Pericyte-derived Bone Morphogenetic Protein 4 Underlies White Matter Damage after Chronic Hypoperfusion**

Corresponding author: Masafumi Ihara, MD, PhD, FACP

Department of Neurology, National Cerebral and Cardiovascular Center Hospital, Osaka, Japan

5-7-1 Fujishiro-dai, Suita, Osaka 565-8565, Japan

FAX: +81-6-6835-5137

TEL: +81-6-6833-5012

E-mail address: ihara@ncvc.go.jp

#### Supplementary Table 1. Primary antibodies used for immunohistochemistry of human brain tissue tissue

Antigen	Host	Dilution	Product Code	Company
ACTA2	Rabbit	1:100	ab5694	Abcam, Cambridge, UK
BMP2	Rabbit	1:200	ab82511	Abcam
BMP4	Mouse	1:100	MAB1049	Millipore, Billerica, MA, USA
BMP6	Mouse	2 µg/ml	MAB1048	Millipore
BMP7	Rabbit	4 µg/ml	ab56023	Abcam
BMP9	Rabbit	1:50	ab35088	Abcam
COL4A1	Rabbit	1:200	ab6586	Abcam
MBP	Mouse	1:200	MA1-10837	Thermo Fisher Scientific, Waltham, MA, USA
PDGFRA	Rabbit	1:150	5241	Cell Signaling, Danvers, MA, USA
PDGFRB	Goat	1:500	AF385	R&D Systems, Minneapolis, MN, USA
TGFB1	Mouse	1:50	sc-146	Santa Cruz, Dallas, TX, USA

#### Supplementary Table 2. Primers used for RT-PCR

Gene	Species	Sequence (5' -> 3')	
<i>Acta2</i>	Mouse	Fw	GGACGTACAACCTGGTATTGTGC
		Rv	TCGGCAGTAGTCACGAAGGA
<i>Bmp4</i>	Mouse	Fw	ATTCCTGGTAACCGAATGCTG
		Rv	CCGGTCTCAGGTATCAAACCTAGC
<i>Gapdh</i>	Mouse/Rat	Fw	TGACGTGCCGCCTGGAGAAA
		Rv	AGTGTAGCCCAAGATGCCCTTCAG
<i>Gfap</i>	Rat	Fw	AGAAAACCGCATCACCATTC
		Rv	GCACACCTCACATCACATCC
<i>Hprt</i>	Mouse	Fw	CTGGTGAAAAGGACCTCTCGAA
		Rv	CTGAAGTACTCATTATAGTCAAGGGCAT

<i>Mbp</i>	Rat	Fw	ACACACAAGAACTACCCACTACGG
		Rv	AGCTAAATCTGCTGAGGGACAG
<i>Pdgfra</i>	Rat	Fw	CTAATTCACATTCCGGAAGGTTG
		Rv	GGACGATGGGCGACTAGAC
<i>Pdgfrb</i>	Mouse	Fw	ACAATTCCGTGCCGAGTGACAG
		Rv	AAAAGTACCAGTGAAACCTCGCTG

**Supplementary Table 3. Primary antibodies used for immunocytochemistry**

Antigen	Host	Dilution	Product Code	Company
Gfap	Rabbit	1:500	Z0334	DAKO, Glostrup, Denmark
Mbp	Mouse	1:200	MA1-10837	Thermo Fisher Scientific
Pdgfra	Goat	1:200	AF1062	R&D Systems
PECAM1	Mouse	1:1000	3528	Cell Signaling

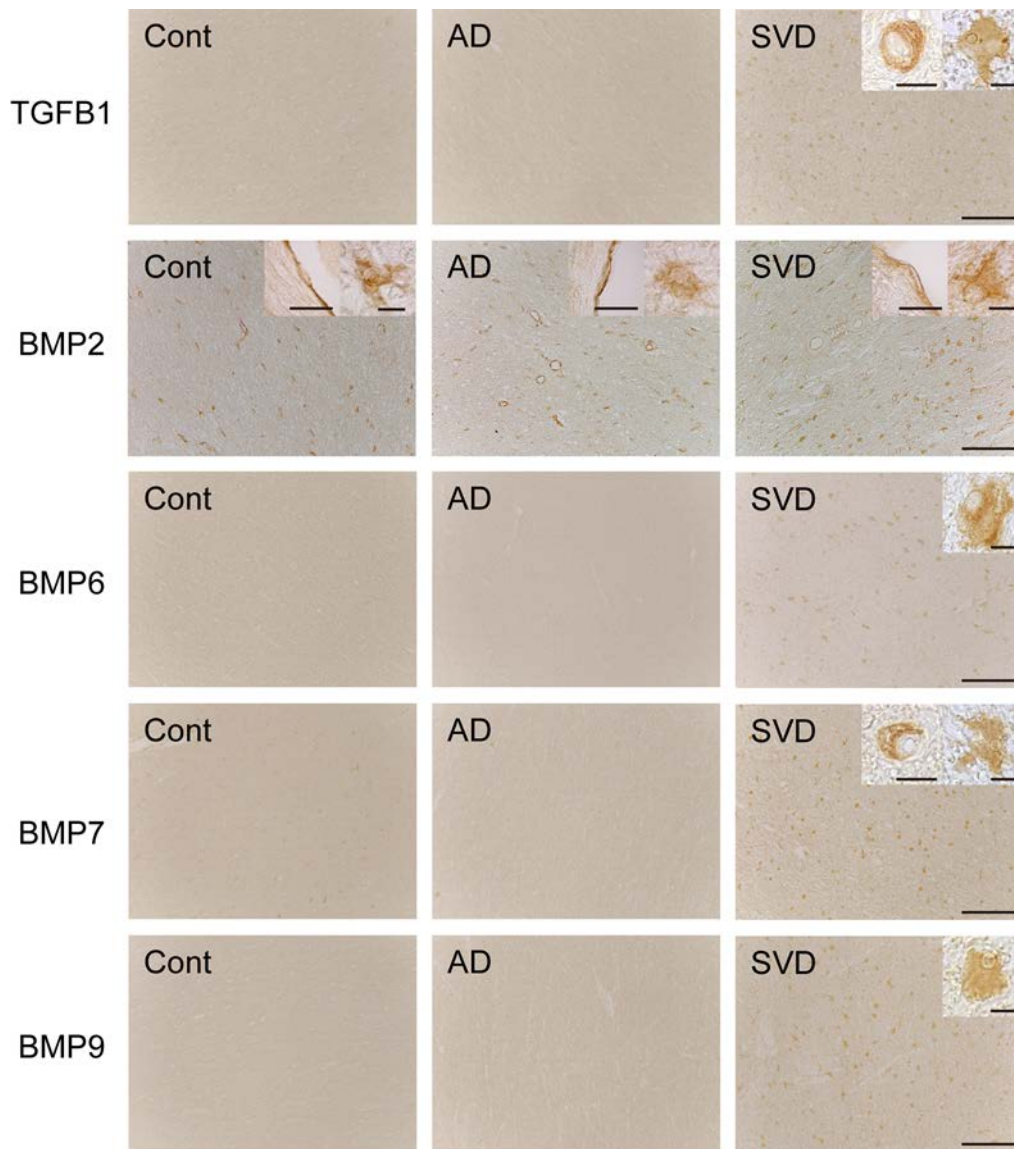
**Supplementary Table 4. Primary antibodies used for immunohistochemistry of mouse brain tissue**

Antigen	Host	Dilution	Product Code	Company
Acta2	Rabbit	1:100	ab5694	Abcam
Bmp4	Mouse	1:100	MBA1049	Millipore
Gfap	Rat	1:200	13-0300	Thermo Fisher Scientific
Mbp	Rabbit	1:200	PD004	MBL, Nagoya, Japan
Olig2	Rabbit	1:500	AB9610	Millipore
Pdgfrb	Goat	1:1000	AF1042	R&D Systems

**Supplementary Table 5. Primary antibodies used for western blot**

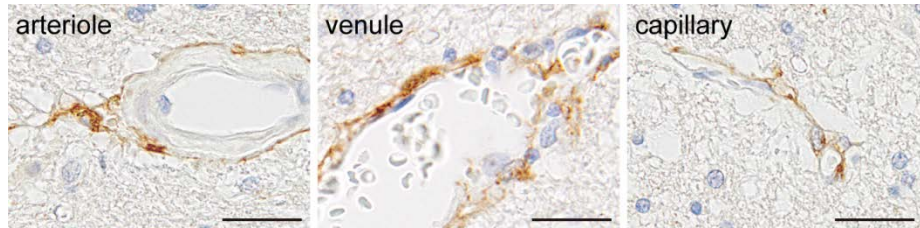
Antigen	Host	Dilution	Product Code	Company
Acta2	Rabbit	1:1000	ab5694	Abcam
*Bmp4	Rabbit	1:1000	ab39973	Abcam
Bmp4	mouse	1:1000	MAB1049	Millipore
Bmp4	mouse	1:1000	sc-393329	Santa Cruz, Dallas, TX, USA
Gfap	Rabbit	1:1000	Z0334	DAKO
Olig2	Rabbit	1:2000	AB9610	Millipore
Pdgfrb	Goat	1:1000	AF1042	R&D Systems
Tubg1	Mouse	1:10000	T-6557	Sigma, Saint Louis, MO, USA

\* used in Fig. 6C and Supplementary Fig. 2A.



**Supplementary Figure 1. Expression of TGFB1, BMP2, BMP6, BMP7, and BMP9 in white matter.**

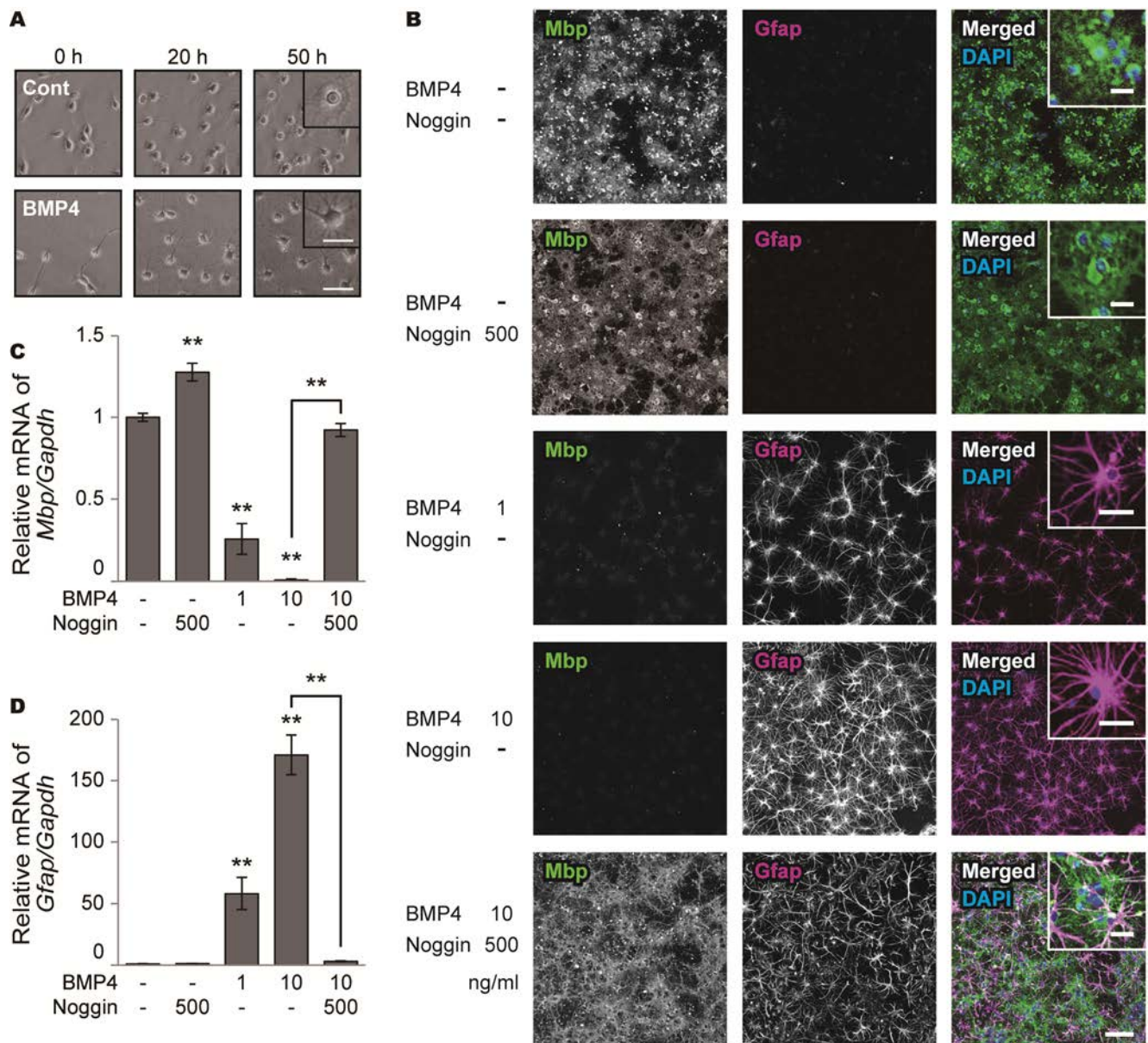
Representative images of TGFB1, BMP2, BMP6, BMP7, and BMP9 staining in the WM of control, AD, and SVD, respectively. Insets show TGFB1, BMP2, BMP6, BMP7, or BMP9-positive activated astrocytes with large cell bodies (right panels), TGFB1 or BMP7-positive pericytes (left panels in TGFB1 and BMP7), and BMP2-positive endothelial cells (left panels in BMP2), respectively. *Bars* indicate 100  $\mu\text{m}$  and 10  $\mu\text{m}$  (insets).



**Supplementary Figure 2. Oligodendrocyte precursor cells in the subventricular zone.** Representative images for PDGFRA-positive cells surrounding arterioles, venules and capillaries in the subventricular zone.

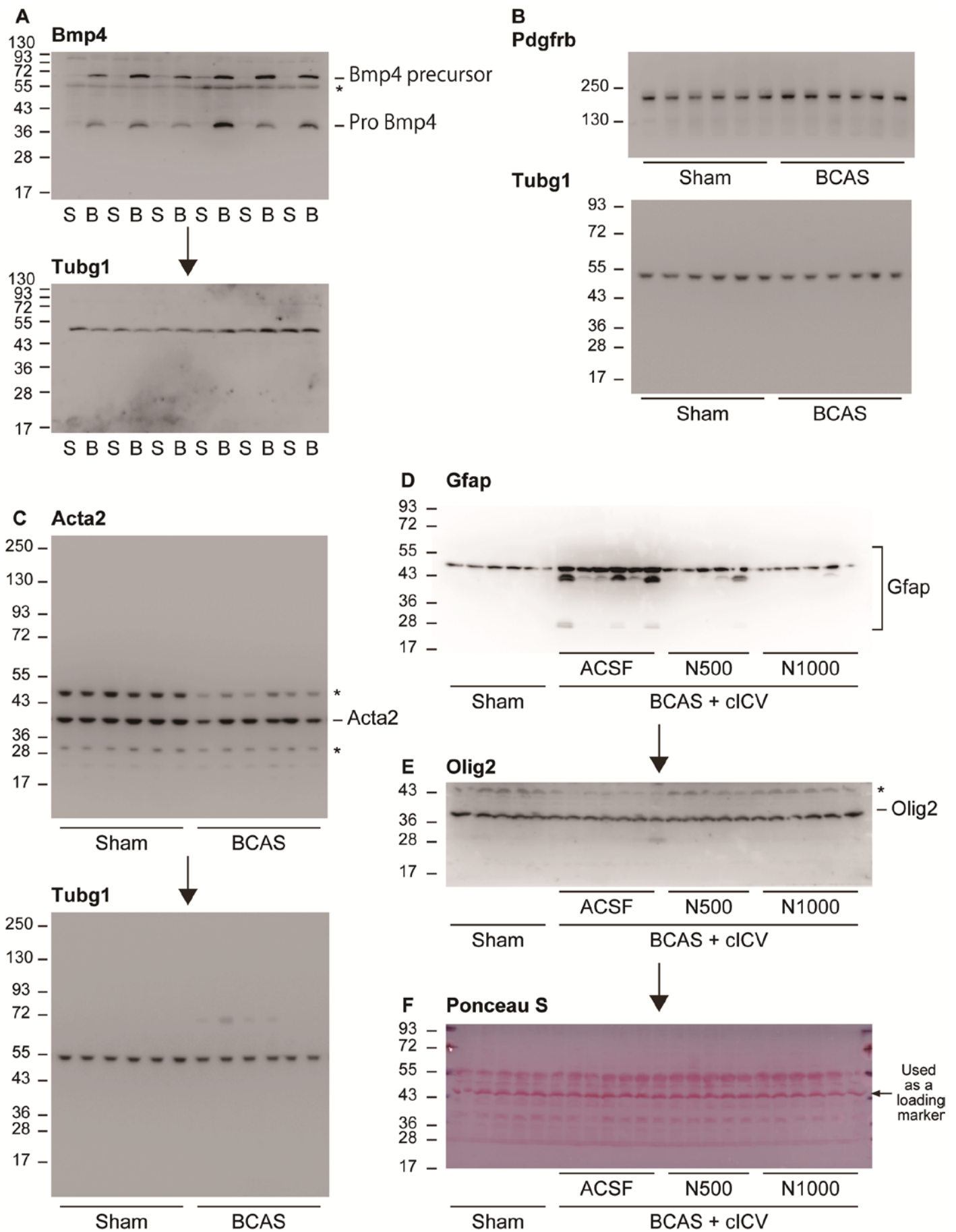
*Bars* indicate 25  $\mu\text{m}$ .





**Supplementary Figure 3. Effects of BMP4 on oligodendrocyte maturation in the OPC differentiation assay.** (A) Time-lapse images of primary OPCs in differentiation media with or without BMP4. Insets show enlarged images. *Bars* indicate 100  $\mu$ m and 50  $\mu$ m (insets). (B) Representative triple-immunofluorescent images for *Mbp* and *Gfap*, and their merged images with DAPI for nuclear staining. Insets show enlarged images. *Bars* indicate 100  $\mu$ m and 15  $\mu$ m (insets). (C, D) Relative mRNA levels of *Mbp* and *Gfap* in the differentiation assay. *Mbp* mRNA levels decrease in differentiation media containing BMP4 (\*\* $P < 0.001$  for 1 and 10 ng/ml) in a dose-dependent manner; the effect of BMP4 is reversed by noggin (\*\* $P < 0.001$ ). Treatment with noggin alone increases *Mbp* (\*\* $P < 0.001$ ) (C). BMP4 significantly increases *Gfap* mRNA expression (\*\* $P < 0.001$  for 1 and 10 ng/ml) in a dose-dependent manner; the effect of BMP4 is canceled out by noggin (\*\* $P < 0.001$ ) (D). *Vertical bars* represent mean  $\pm$  SD. Abbreviation is as follow: Cont,

control; Gapdh, glyceraldehyde-3-phosphate dehydrogenase.



**Supplementary Figure 4. Original gel pictures for western blots.** The figure shows uncropped western blots displayed in Fig. 6C. (A) Bmp4 precursor and pro-Bmp4 expressions are increased in BCAS mice



compared with sham controls. *Pdgfrb* (B), but not *Acta2* (C), expression is increased in BCAS mice compared with sham controls. Each band of *Bmp4*, *Pdgfrb*, and *Acta2* is normalized to *Tubg1*. (D) *Gfap* expressions are increased in BCAS mice compared with sham controls, which are suppressed by noggin cICV (500 ng/day and 1000 ng/day). (E) *Olig2* expressions are decreased in BCAS mice compared with sham controls, which are ameliorated by a high dose of noggin cICV (1000 ng/day). (F) Each band of *Gfap* and *Olig2* is normalized to the band at 45 kDa stained with ponceau S. Asterisks show unknown bands. Abbreviations are as follows: B, BCAS; N500, Noggin 500 ng/day; N1000, Noggin 1000 ng/day; S, Sham operation.